Multiparameter-analysis of CO_2/Steam-enhanced gasification and pyrolysis for syngas and biochar production from low-cost feedstock

Rafael B.W. Evaristo [a], Ricardo Ferreira [b], Juliana Petrocchi Rodrigues [c], Juliana Sabino Rodrigues [e], Grace F. Ghesti [a,*], Edgar A. Silveira [d,*], M. Costa [b]

[a] Laboratory of Brewing Bioprocesses and Catalysis to Renewable Energy, Chemistry Institute, University of Brasilia, Brasilia, DF 70910-900, Brazil
[b] IDMEC, Mechanical Engineering Department, Instituto Superior Técnico, Universidade de Lisboa, Lisboa, Portugal
[c] Faculty of Gama, University of Brasília, Brasília, DF 70910-900, Brazil
[d] Mechanical Engineering Department, University of Brasília, Brasília, DF 70910-900, Brazil
[e] Forest Products Laboratory, Brazilian Forest Service, Brasília 70818900, Brazil

ARTICLE INFO

ABSTRACT

The disposal of spent coffee grounds (SCG) and brewers' spent grains (BSG) has become an environmental issue. Thus, the waste-to-energy valorization of these two low-cost feedstocks was performed via gasification and pyrolysis to assess their potential as syngas and biochar fuels. The processes' optimum conditions were investigated by a multiple-criteria decision support method. Firstly, both raw materials were gasified at 1000 °C with O_2/N_2, $O_2/CO_2/N_2$ and $O_2/H_2O/N_2$ atmospheres. The characteristics and energy performance of the producer gas were evaluated. In addition, the exergy analysis of green-H_2 production was assessed. The pyrolysis experiments were conducted at 300, 500 and 700 °C, followed by a comprehensive characterization of the biochar properties and its combustion behavior. The syngas production based on CO_2/Steam-enhanced gasification has indicated clear energetic and exergetic improvements against O_2/N_2 with a promising increase of 32.97% LHV_{syngas} for BSG. Obtained biochar possesses favorable fuel characteristics promoting an HHV enhancement up to 19.42% (SCG) and 83.11% (BSG). Furthermore, the combustion index indicated a great potential of using SCG and BSG as solid biofuel for straightforward application to heat generation in small-scale systems. Therefore, syngas and biochar characteristics encourage feasible biofuels from low-cost feedstocks for energy generation.

Introduction

The human population reached a new height of 7.8 billion in recent years, boosting the ever-growing food, energy and other resources demands [1]. As a result, the world's energy consumption reached 14 billion tons of oil equivalent, requiring efforts to mitigate environmental impacts and higher investments in renewable and sustainable energies to fulfill fossil fuel demands [2,3].

In Brazil, the massive agroindustry of coffee has grown its economic contribution to exportation and the internal market. Coffee is the second most popular drink globally consumed, producing a substantial amount of valuable organic waste known as spent coffee grounds (SCG) [4]. The process of coffee beverage preparation regularly produces substantial SCG and has increased its generation from 8.8 million tons in 2014 to 9.3 million tons in 2017, provoking disposal issues and leading to environmental concerns [5]. About 650 kg of SCG are generated from 1 ton

of green coffee bean, and about 2 kg of wet SCG are obtained from 1 kg of soluble coffee during preparation [6].

The high carbon content, higher heating value (HHV), low ash, and negligible sulfur content of SCG make it an alternative fuel source through thermochemical conversion [7]. Furthermore, the integration with biorefinery in general and with pyrolysis process in specific is considered the most successful solid waste management strategy of SCG that produces energy and high-value products [4].

In recent years, the beverage sector, especially the beer segment, showed a tremendous economic impact in all Brazilian states. About 14 billion liters of beer are produced annually in Brazil, occupying third place in the list of world producers, standing behind only by China and the USA, respectively, with a 5% share of the world beer market [8]. With the growth of the Brazilian beer market, it was observed that, for the most part, start-up companies are small and medium-sized [9].

The brewing industries produce millions of tons of residues, which in the context of a linear economy approach will end up in landfills

Nomenclature

Index summary

d_n	Metric
β	biomass correlation factor
BSG	brewers' spent grains
CCE	carbon conversion efficiency
CEI	carbon enhancement index
CGE	cold gas efficiency
CO	carbon monoxide
CO_2	carbon dioxide
D_f	burnout index
D_i	ignition index
DA	dominance analysis
DTG	thermogravimetric derivative
$Ex_{biomass}$	exergy of biomass
Ex^{ch}	chemical exergy
Ex^{ki}	kinetic exergy
Ex^{ph}	physical exergy
Ex^{po}	potential exergy
E_{CO_2}	gasificaiton CO_2 emission
EF	enhancement factor
EMCI	energy-mass-coefficient -index
$ex^{ch}_{H_2}$	standard chemical exergy
Ex_{H2}	exergy of hydrogen
EY	energy yield
h	specific enthalpy
h_0	specific enthalpy
HHV	higher heating value
LHV	lower heating value
$\dot{m}_{bio}$	biomass feeding rate
n	molar yield
η_{H_2}	exergy efficiency of hydrogen
Q	syngas flow rate
r_i	mole fraction
S	combustion index
s	specific entropy
s_0	specific entropy at T_0
SCG	spent coffee ground
SD	strong dominance
SEM	Scanning Electron Microscope
SY	solid yield
S/B	steam to biomass ratio
γ_{syngas}	syngas yield
T	Temperature
t	Time
T_0	temperature of environment
T_f	burnout temperature
T_i	ignition temperature
T_p	peak temperature
TGA	thermogravimetric analysis
t_f	burnout time
t_i	ignition time
t_p	peak time
$w_{biochar}$	biochar weight
$w_{initial}$	raw biomass weight
WD	weak dominance
WTE	waste-to-energy
$x_{carbon,i}$	carbon molar fraction
y_{carbon}	feedstock carbon mass fraction
y_{CO} or y_{H_2}	CO or H_2 percentage in syngas

representing a management issue from ecological and economic points of view [10]. Brewers' spent grains (BSG) are the primary solid residue of beer production and corresponds to 93% of the total mass of the waste. On average, 14–20 kg of dry BSG is generated for 100 L of produced beer [11]. Consequently, with the growth in beer production, there is also an increase in residues.

A new perspective allows seeing wastes as low-cost resources, useful for other processes, within or without the industry that produces them [5,12]. Move toward the circular economy principles could save up to 20% of the costs for numerous industrial sectors such as beverages, food, textiles and packaging [13]. Therefore, waste-to-energy systems can be suitable for converting waste into usable energy within a circular economy [13–15].

Thermo-chemical processes convert solid organic feedstocks into three-phase pyrogenic products such as biochar, bio-oil, and syngas [13,16–18]. Biochar as solid biofuel is among the least studied, although its logistical advantages (reliable production, straightforward application and storage-ability) [19,20]. Typically, biochar has superior properties such as low heterogeneity, high calorific values, high combustibility, low moisture content, and grindability than raw biomass as solid fuels [21–23]. Therefore, in the present research stage, it is essential to supply biochar feedstock that satisfies some criteria such as low-cost source, renewable in nature, and long-term sustainability.

The SCG is a residue rich in carbon and can be used as a substrate for biochar production. Due to its characteristics, pyrolysis technology is the preferred thermo-chemical procedure and has one of the most promising potentials for the valorization of SCG due to its high-quality conversion and yield of solid products [4].

Tsai et al. (2012) produced the biochar with high carbon content and calorific value by using SCG as a feasible raw material at a fixed heating value [24]. The carbon content was >80 w/w%, and the calorific value was more significant than 30.1 MJ.kg^{-1} [24]. Vardon et al. (2013) assessed SCG for biodiesel, bio-oil, and biochar. Their biochar obtained at 450 °C reported an HHV of 31.0 MJ.kg^{-1} showing its potential to be co-fired as a solid fuel with an energy density comparable to solid fossil fuels [25]. Li et al. (2014) investigated the pyrolysis efficiency of SCG, showing promising results with 77 and 85% efficiency at the heating rates of 10 and 60 °C min^{-1}, respectively [26]. Matrapazi et al. (2020) conducted pyrolysis experiments on SCG between 430 and 760 °C with a 50 °C.s^{-1}, obtaining the product yields, composition and calorific values and allowing a Techno-economic study [27]. Finally, Lee et al. (2021) evaluated SCG as a potential feedstock for solid biofuel production to reduce solid waste and generate value products [1]. The combustion kinetics was investigated, and optimized SCG-biochar showed favorable fuel characteristics such as high fixed carbon content (82.83%), low volatile matter (12.28%) and low ash content (2.22%) [1].

The use of BSG in thermochemical conversion processes has been assessed because of its encouraging potential within the circular economy principles [28,29]. The valorization of BSG has been investigated, focusing on bio-oil [30–32] and activated carbons products [33], description of thermal decomposition kinetics [31,34], as well as the biochar properties [30,35] and absorption purposes [36].

Sanna et al. (2011) investigated the pyrolysis of BSG between 460 and 540 °C using an activated alumina bed [30]. Results showed that despite the high nitrogen content on raw BSG material, the process left a bio-oil with less nitrogen of 68% at 460 °C compared to 82% at 520 °C [30]. In contrast, a higher proportion of nitrogen remains in the biochar at 460 °C, indicating that the biochar can be used as a soil amendment and carbon sequestration agent [30]. Machado et al. (2020) explored the 500–700 °C pyrolysis temperatures, describing product yields and

biochar properties focusing on adsorption purposes. Finally, centering on bio-oil and biochar products from BSG, Borel et al. (2020) investigated the effects of pyrolysis temperature and heating rate within a fixed-bed tubular reactor [35]. Their results showed a biochar product that could be applied as a biofuel due to its high HHV (27.1–28.3 kJ. g^{-1}), moderate ash content (11.5%) and low sulfur content (<0.6%) [35].

The thermochemical process may not require a pretreatment because C, H and O elements of cellulose, hemicellulose, lignin, lipid, and protein can be thermally degraded and ultimately converted into syngas (H$_2$ + CO) via gasification [37]. Thus, controlling H$_2$/CO ratios and other operating conditions, syngas can be directly employed as a fuel and/or used as an intermediate for synthesizing more value-added chemicals [38]. In addition, it is known that CO$_2$ generated from biomass valorization can be used for the re-growth of biomass, making the entire process carbon–neutral [37].

As an alternative for energy generation from residues of the coffee harvest, gasification was extensively reviewed by Martinez et al. (2021), showing few studies focusing on the coffee pulp [39,40], husks [41–44] and SCG [45]. In addition, recent studies on SCG gasification described the kinetic modeling of CO$_2$ gasification for SCG biochar [46], the two-step gasification of SCG biochar for hydrogen-rich gas production [47], the thermal behavior and product yield of SCG steam catalytic gasification [48] and the steam and CO$_2$ gasification under different concentrations [7].

Concerning BSG, the gasification literature review presents few studies. Ferreira et al. (2019) pointed out that the literature about BSG through pyrolysis and gasification processes is very scarce [38,49]. Ferreira et al. (2019) investigated allothermal steam gasification of BSG to obtain a combustible gas. The process performance was assessed by evaluating the cold gas (47.0%–52.1%) and carbon conversion (57.0%–62.7%,) efficiencies showing a sufficient quality to satisfy energy needs. Another work investigates BSG gasification in a downdraft reactor conducting experiments and performing numerical modeling with a stoichiometric equilibrium model [38]. The study evaluated the syngas quality employing the gas yield, lower heating value, carbon conversion efficiency, and cold gas efficiency [38]. The results showed that gasification provides a producer gas with enough quality for energy production in boilers or turbines using air as a gasifying agent [38].

Due to the limited studies focusing on energy generation from coffee and beer production chain residues, only partial information describing the thermochemical process implementations on coffee and beer residues is available [50]. It is essential to point out that investigating residues from agro-industrial activities is surprisingly less common in the literature, even though they represent a significant amount of material with potential energy recovery by gasification [46]. Furthermore, as shown in Table S1 (supplementary material), the studies focusing on transforming SCG and BSG into prospective solid biofuels (biochar) by slow pyrolysis and applying different gasification agents are still limited in the current literature.

Thus, considering this massive potential and continuous supply of BSG and SCG wastes and the perspective to achieve sustainable energy recovery from those waste, the objective of this study was to investigate their potential as low-cost feedstocks for energy production by thermochemical processes: pyrolysis and gasification. For this purpose, a comprehensive characterization was performed for steam/CO$_2$-enhanced gasification and pyrolysis processes.

First, gasification experiments contemplated three different operational conditions for SCG and BSG followed by a detailed characterization of the syngas composition, energy properties (LHV, cold gas efficiency, carbon conversion efficiency and syngas yield) and green hydrogen exergy efficiency. Next, the biochar production was investigated with three treatment temperatures (300, 500 and 700 °C). After that, the biochar product was physically characterized by its yield (BY) and SEM analysis and chemically assessed by ultimate composition (C, H, O and N) and energy aspects (HHV, energy yield and its enhancement factor and energy-mass co-benefit index).

Finally, the syngas and biochar products were submitted to a multi-criteria decision analysis revealing and ranking the optimum operation conditions based on the discussed performance indicators. In addition, the combustion behavior of raw SCG and BSG and derived biochar were investigated with thermogravimetric analysis, revealing its potential as a solid fuel for straightforward application.

The meaningful results of this work could assist decision-makers in proposing optimum routes to the more economic valorization of SCG and BSG through pyrolysis and gasification treatments. Currently, these residues have been discarded in landfills generating an environmental liability. The cost for correct disposal is high and depends on the availability of receiving inputs. Furthermore, the proposed methodology can be extended for further thermochemical route valorization with low-cost feedstock, boosting waste-to-energy development and circular economy principles.

Material and methods

Feedstock

The BSG was obtained from the Stadt Brewery located in Goiás, in Brazil's central region. The SCG, supplied by a local coffee brand (café export), is composed of Arabica species of coffee. The biomass residues were oven-dried (105 °C for 24 h), ground in a mill and sieved (60–80mesh) for the thermochemical processes and physicochemical characterization.

Chemical analysis

The chemical characterization was conducted for SCG and BSG raw feedstock and pyrolyzed material. The proximate analysis was evaluated according to ASTM D 5142-09 standard. The ash content was inferred based on the TAPPI T211 om-93 standard [51]. Soluble and insoluble lignin contents were determined using laboratory analytical procedures from the National Renewable Energy Laboratory (NREL, LAP 003, and 004/1995). Moreover, total extractives were quantified in ethanol: toluene (2:1, v/v) according to TAPPI Standards & Methods (T 204 om-88), with adaptations [52]. Finally, the holocellulose content without extractives was calculated by subtracting the total lignin and ash content.

The changes in the surface morphology were investigated using Scanning Electron Microscope (SEM) with the TM-4000Plus from Hitachi, Japan. The sample images were captured using a voltage of 15 kV and 400X and 1000X magnification. The ultimate analysis was performed using an EA 2400 series II analyzer, from Perkin Elmer, with acetanilide as standard [45,46]. Other components were determined using a Shimadzu X-ray Fluorescence (XRF) spectrometer (model EDX 720) with Rhodium tube as X-ray source.

The higher heating values (HHV) were estimated through the modified Dulong's formula (Eq. (1)) [53,54]:

$$HHV = (0.3393 \times C) + [1.443 \times (H - O/8)] + (0.01494 \times N) \qquad (1)$$

The LHV was calculated through Eq. (2) [55]:

$$LHV_{biomass} = HHV - 21.97 \times H \qquad (2)$$

In this work, the pyrolysis treatment was evaluated by the carbon element index (CEI), thus allowing a dimensionless (0–1) parameter to account for process performance [56]. The CEI (Eq. (3)) is defined as a function of the weight extent of carbon in the feedstock (CE_{raw}), in the different biochar products (CE_i, where i = raw, $biochar_{300°C}$, $biochar_{500°C}$, and $biochar_{700°C}$) and in the most severe treatment ($CE_{biochar_{700°C}}$) [56].

$$CEI = \frac{CE_i - CE_{raw}}{CE_{biochar_{700°C}} - CE_{raw}} \qquad (3)$$

The obtained chemical properties of raw SCG and BSG are summarized in Table 1.

SCG and BSG gasification

The experimental gasification setup, comprehensively described in the previous works [57–59], is illustrated in Fig. 1. The gasification system comprises a biomass feeder, a vertical electrically heated drop tube reactor (DTR) (12 kW), a particle collection system, and a gas supply, sampling and analysis system [57,58].

Gasification operational conditions were defined based on previous studies [57–59]. Three distinct gasification mediums (O_2/N_2, $O_2/CO_2/N_2$ and $O_2/H_2O/N_2$ [57]) and one temperature (1000 °C [7,57–61]) were evaluated for both biomass feedstock (SCG and BSG). Biomass was constantly feeding into the reactor with a constant rate equal to 0.03 and 0.024 kg.h^{-1} for SCG and BSG, and the residence time was 10 min.

The gasifying agent stream comprises pure N_2, pure O_2 and steam, or CO_2, blended on the desired proportion. The oxygen equivalence ratio, λ (the ratio between the oxygen fed and the stoichiometric oxygen needed for the biomass oxidation), was established as 0.4 based on the previous work [58,59]. The total inlet gas flow was 1 dm^3.min^{-1}, being N_2 used to balance [58,59]. The O_2 flow rate was 0.11 L.min^{-1}, and the inlet concentrations of both CO_2 and H_2O were also kept constant (5 vol%).

The composition of the produced syngas (H_2, CH_4, CO_2 and CO) was quantified using a non-dispersive infrared analyzer for CO_2 and CO, a paramagnetic pressure analyzer for O_2, and a gas chromatograph Clarus 500 for the remaining gases [57]. The following performance indicators were calculated to identify the optimum conditions of gasification processes for both low-cost feedstocks: syngas yield (γ_{syngas}), carbon conversion efficiency (CCE), cold gas efficiency (CGE), lower heating value
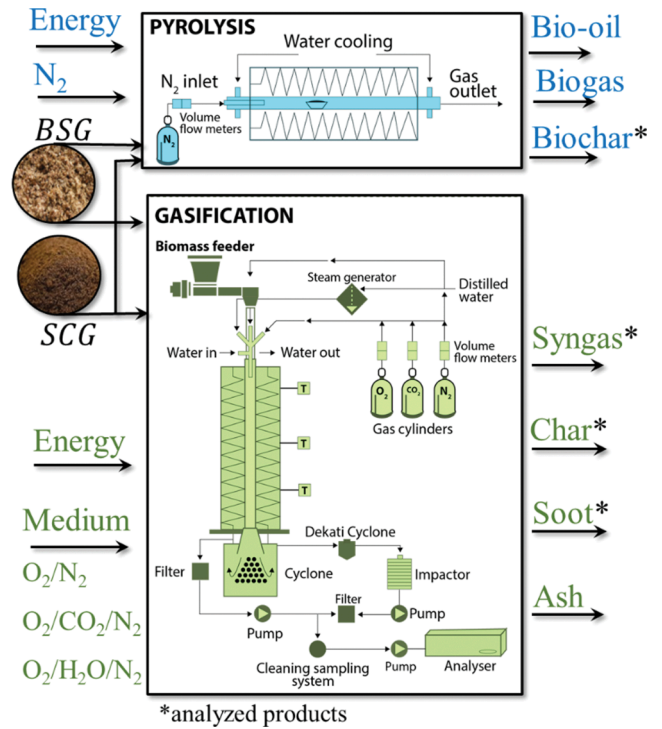

Fig. 1. SCG and BSG thermochemical conversion diagram. (1-column fitting).

of the syngas (LHV_{syngas}) and the exergy efficiency of hydrogen production (η_{H_2}) [54,55,57,61,62].

The CGE and CCE were defined as Eqs. (4) and (5) [57,63]:

$$CGE = \frac{Q_{syngas} \times LHV_{syngas}}{\dot{m}_{bio} \times LHV_{bio}} \quad (4)$$

$$CCE = \frac{Q_{syngas} \times \sum_i^n x_{carbon,i}}{\dot{m}_{bio} \times y_{carbon}} \quad (5)$$

where the $\dot{m}_{bio}$ is the biomass feeding rate (kg.h^{-1}) (Table 2), y_{carbon} is the carbon mass fraction (biomass ultimate analysis in Table 1), $LHV_{biomass}$ are the low heating values of biomass (MJ.kg^{-1}) (Eq. (2)), Q_{syngas} is the syngas flow rate (Nm^3.h^{-1}), and x_{carbon} is the carbon molar fraction in the producer gas products, including carbon in CO, CO_2, and CH_4 [57,63]. The LHV_{syngas} was determined in terms of the mole fraction (r_i) of a constituent i of dry fuel gas and the lower heating value (LHV_i) of the syngas constituents (i = H_2, CH_4, and CO) using Eq. (6) [64]:

$$LHV_{syngas} = \sum r_i LHV_i \quad (6)$$

Table 1
The physical aspect, proximate, lignocellulosic, ultimate analysis, EDX and energy parameters for SCG and BSG raw material.

Feedstock	SCG	BSG
Aspect		
Proximate analysis (wt%)[a]		
Ash	1.67	3.58
Fixed carbon	17.71	16.13
Volatile Matter	80.62	80.29
Moisture	5.47	76.87
Lignocellulosic analysis (wt%)		
Holocellulose	58.58	44.11
Lignin	16.54	34.03
Extractives	21.06	18.67
Ultimate analysis (wt%)[b]		
C	57.74	44.72
H	7.22	6.86
N	2.39	3.21
O[b]	38.65	44.66
S	–	0.55
EDX (mg/kg$_{biomass}$)		
Ca	791	877
K	4201	875
Mg	696	345
Na	122	1203
P	123	563
Si	65	378
Energy parameters		
Formula	CH$_{1.67}$O$_{0.56}$	CH$_{1.83}$O$_{0.75}$
HHV (MJ.kg^{-1})[c]	21.04	17.06
LHV (MJ.kg^{-1})[c]	19.45	15.56

[a] dry basis.
[b] by difference O = 100 − (C + H + N + S).
[c] calculated.

Table 2
Reference value (z_m) of Metric Distance (d_n) decision analysis.

Process	Reference value z_m	
Gasification	SCG	BSG
LHV_{syngas}	0.089	0.055
CGE	0.006	0.006
CCE	0.005	0.007
y_{syngas}	0.014	0.015
η_{H_2}	0.037	0.036
E_{CO_2}	0.411	0.193
Pyrolysis	SCG	BSG
H/C	0.242	0.524
O/C	0.183	0.114
HHV	0.040	0.032
EF	0.837	0.546
EY	0.031	0.020

The γ_{syngas}, defined as the amount of H_2 and CO generated during the process of gasification (mol syngas.kg$_{biomass}^{-1}$), is calculated as Eq. (7) [57]:

$$\gamma_{syngas} = \frac{(Q_{syngas} \times y_{CO}) + (Q_{syngas} \times y_{H_2})}{\dot{m}_{bio}} \qquad (7)$$

Hydrogen production from steam gasification of biomass has been recently studied from the exergy aspect [54,55,61,65]. Therefore, this study applies the exergy efficiency of hydrogen production as a gasification performance indicator to compare and define the optimum condition of gasification processes for the different process atmospheres and biomasses. The exergy of hydrogen (Ex_{H_2}) in kJ.kg^{-1} includes four forms [55]:

$$Ex_{H_2} = Ex^{ph} + Ex^{ch} + Ex^{ki} + Ex^{po} \qquad (8)$$

Here, the kinetic (Ex^{ki}) and potential (Ex^{po}) exergy, which are minimal parts of the total exergy, are neglected [66]. The physical (Ex^{ph}) and chemical (Ex^{ch}) exergy of H_2 (kJ.kg^{-1}) are calculated through Eqs. (9) and (10) [54,67]:

$$Ex^{ph} = n \times [(h - h_0) - T_0 \times (s - s_0)] \qquad (9)$$

$$Ex^{ch} = n \times ex_{H_2}^{ch} \qquad (10)$$

where n is the molar yield of H_2 (mol.kg^{-1}), h the specific enthalpy of H_2 at arbitrary temperatures (kJ.kmol^{-1}); h_0 the specific enthalpy of H_2 in the environment (7926 kJ.kmol^{-1}); T_0 the environmental temperature (298.15 K); s the specific entropy of H_2 at arbitrary temperatures (kJ. kmol^{-1}.K^{-1}) and s_0 the specific entropy of H_2 in the environment (107.71 kJ.kmol^{-1}.K^{-1}); $ex_{H_2}^{ch}$ the standard chemical exergy of H_2 (236100 kJ.kmol^{-1}) [54]. The chemical exergy of both biomasses' feedstock ($ex_{biomass}$) can be defined in function of the correlation factor β and the LHV of raw biomass (kJ.kg^{-1}) according to Eqs. (11) and (12) [9]:

$$ex_{biomass} = \beta \times LHV_{biomass} \qquad (11)$$

$$\beta = \frac{1.044 + 0.0160 \times H/C - 0.3493 \times O/C(1 + 0.0531 \times H/C) + 0.0493 \times N/C}{1 - 0.4124 \times O/C} \qquad (12)$$

where, $ex_{biomass}$ is described as the exergy of biomass (kJ.kg^{-1}) and the C, H, O and N are the weight fraction (%) of biomass feedstock in terms of carbon, hydrogen, oxygen, and nitrogen, respectively. The exergy efficiency of hydrogen production can be defined by Eq. (13) [54,67]:

$$\eta_{H_2} = \frac{Ex_{H2}}{Ex_{biomass}} \times 100\% \qquad (13)$$

The thermochemical conversion of biomass has CO_2 as its main by-product. Therefore, it is crucial to mitigate its emission or recycle it as a gasifying medium, reducing its release [7]. Accordingly, the CO_2 emission per the produced syngas (CO + H_2) was evaluated for both biomasses to gain insight into the relative effect of the process on greenhouse gas emission and/or determine CO_2 production potential to be applied as feedstock for CO_2-enhanced gasification (recycling). The dimensionless E_{CO_2} of the conducted gasification experiments is defined by Eq. (14) [68]:

$$E_{CO_2} = \frac{n_{CO_2}}{n_{CO} + n_{H_2}} \qquad (14)$$

where n is the molar yield of CO_2, CO and H_2 (mol.kg^{-1}).

Pyrolysis

The pyrolysis apparatus exhibited in Fig. 1 consisted of an alumina recrystallized horizontal tube (inner diameter of 4 cm) placed inside an electrically heated furnace (4 kW) with a water-cooled vessel [69]. An S-type thermocouple continually monitored the temperature of the reactor system [69]. Nitrogen gas at 1 dm^3.min^{-1} supplied an inert atmosphere during treatment. For each experiment, biomass samples of $\approx$ 3 g were used.

The oven-dried samples were positioned within the horizontal tube and heated with a 33 °C min^{-1} heating rate from room temperature until the desired pyrolysis temperature (300, 500, and 700 °C) and kept isothermally for 60 min. The experiments were conducted in duplicate for each operational condition. The biochar yield (BY) was obtained by Eq. (15) [70–73].

$$BY = \frac{w_{biochar}}{w_{initial}} \times 100\% \qquad (15)$$

Here, $w_{biochar}$ is the weight of the obtained biochar and $w_{initial}$ the initial biomass weight. The energy yield (EY) of biochar was calculated considering the HHV enhancement factor (EF) and the BY for each pyrolysis condition as Eqs. (16) and (17), respectively [23,74,75].

$$EY = EF \times BY \qquad (16)$$

$$EF = \frac{HHV_{biochar}}{HHV_{raw}} \qquad (17)$$

The difference between the energy yield and the solid yield is defined as the energy-mass co-benefit index (EMCI) [76,77] and can be used as a performance value to establish the optimum operating condition for biomass pyrolysis [78,79]. The EMCI is determined with Eq. (18) [22,78–80]:

$$EMCI = EY - BY \qquad (18)$$

Thermogravimetric analysis (TGA)

The thermogravimetric combustion experiments were conducted with a Shimadzu DT-60 TGA. The experiments were performed for SCG and BSG biochar products (300, 500 and 700 °C) under air atmosphere (30 ml.min^{-1}). The samples (4 ± 0.1 mg) were heated with linear heating of 20 °C.min^{-1} from room temperature to 1000 °C. The experiments were performed in duplicate to verify reproducibility.

The combustion characteristic of SCG and BSG biochar products were evaluated by combustibility indexes such as the ignition index D_i (%.min^{-3}) and the burnout index D_f (%.min^{-4}) [81,82]. In addition, and the characteristic combustion index S (%$^{-2}$.min^{-2}.°C^{-3}) was assessed [83]. The combustion performance indicators are defined by Equations (19–21).

$$D_i = \frac{DTG_{max}}{t_p \times t_i} \qquad (19)$$

$$D_f = \frac{DTG_{max}}{\Delta t_{1/2} \times t_p \times t_f} \qquad (20)$$

$$S = \frac{DTG_{max} \times DTG_{mean}}{T_i^2 \times T_f} \qquad (21)$$

Here, the ignition temperature T_i (°C) describes the temperature at which a material starts burning and can be determined by TG–DTG tangent method [84]. The peak temperature T_p (°C) is the temperature corresponding to the peak of the maximum DTG value (DTG_{max}). The burnout temperature T_f (°C) is taken as the point immediately before the combustion reaction is completed, when the rate of weight loss becomes less than 2%. min^{-1} of DTG [81]. The time in which the ignition, peak and burnout temperatures occur are t_i, t_p and t_f (min), respectively. The DTG_{mean} is the average combustion rate considering the 1% of the DTG_{max} as the start and the end of the process. $\Delta t_{1/2}$ is the time range of $\frac{DTG}{DTG_{max}} = 0.5$ [85].

Decision analysis for optimized biofuel

Usually, a decision problem accounts for several targets, so the most satisfactory solution to the problem is investigated considering several criteria [69]. Understanding that there is no global solution for all products concurrently, and multiple solutions can be achieved for different purposes, a decision analysis must be applied to select the ideal process variables. Therefore, in the present study, the decision analysis is performed by applying two methods: Dominance Analysis (DA) and Metric Distance (d_n) based on compromise programming [47]. The DA method can be described by Eq. (22) [69].

$$x_1 \leq x_2 iff \begin{cases} f_i(x_1) \leq f_i(x_2) \forall i \in 1, \cdots, p \\ \exists j \in 1, \cdots, M f_i(x_1) \leq f_i(x_2) \end{cases} \quad (22)$$

Wherein a problem with p decision criteria $f_m = \{f_1(x_n), f_2(x_n), \cdots, f_M(x_n)\}$ and a set of N solutions $x_n = \{x_1, x_2, \cdots, x_N\}$, solution x_1 dominates solution x_2 if and only if x_1 is not worse than x_2 in all criteria and x_1 is strictly better than x_2 in at least one criteria [69]. A solution dominates others strongly (SD) if it has a better or equal result in all criteria [69]. A solution dominates others weakly (WD) if it has a better result in at least one criterion [69].

Given a reference point (z_m), the compromise programming method benefits a solution closer to the desired value or farther to an undesired value [86]. The metric distance (d_n) of a solution n (Equation (23)) represents the distance (measured by a specific vector – the Euclidean distance) between the solution n and z_m in the solutions space.

$$d_n = \left[\sum_{m=1}^{M} |f_m(x_n) - z_m|^p \right]^{1/p} \quad (23)$$

Here, M is the number of all solutions and $f_m(x_n)$ is the value of solution n in the criterion m. The best solutions have shorter distances between them and a reference desired solution [86]. The reference point represents the coordinates of the preferred values of all the criteria presented for each product: biochar and syngas (biofuel) [69]. The reference value z_m (Table 2) is defined considering the advantages for each specific parameter, based on the raw biomass and product characterization, and the described performance indicators for gasification and pyrolysis processes in Section 2.2 and 2.3 and results in Section 3 [69]. Table 2

The decision was straightened as a minimization problem for both methods, where the evaluated criteria are seen as benign when lower (or minimized) [69]. Hence, the best (to be) higher criteria were dealt with as the numeric inverse (1/higher = lower) [69]. The values presented in Table 2 follow this criterion.

Results and discussions

Gasification

Fig. 2(a and b) show the producer gas composition (H_2, CO, CO_2, and CH_4) for SCG and BSG for the conventional (O_2/N_2) and CO_2/Steam-enhanced gasification ($O_2/CO_2/N_2$ and $O_2/H_2O/N_2$). The presented syngas concentrations were calculated using an N_2 free basis. Fig. 2(c)
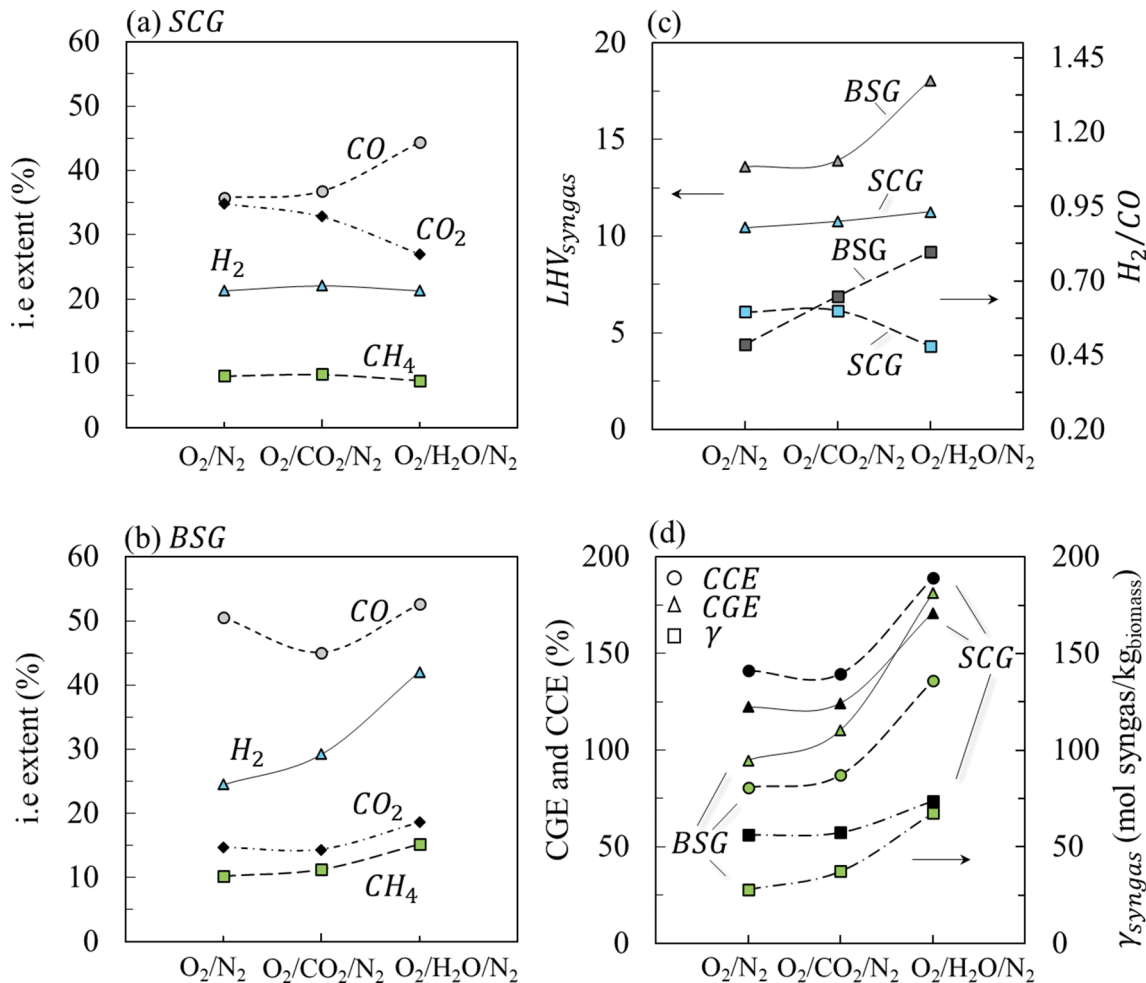

Fig. 2. Producer gas composition for SCG (a) and BSG (b). (c) H_2/CO ratio and LHV_{syngas} and (d) CGE, CCE and Syngas yield (γ_{syngas}) as a function of the gasification gas medium. (2-column fitting).

provides the calculated LHV_{syngas} and H_2/CO ratio, while Fig. 2(d) evaluated the CGE, CCE and γ_{syngas} for the three gasification mediums.

The producer gas composition of SCG gasification with $O_2/CO_2/N_2$ evidenced a minor increase of 3.77, 2.94 and 2.8% for H_2, CH_4 and CO, respectively, compared to O_2/N_2. On the other hand, the CO_2 relative content, with 32.81%, reduced 5.86% compared to O_2/N_2 results. This behavior might be attributed to the char reactions ($C + CO_2 \rightarrow 2CO$) and CO_2 reforming reactions ($C_xH_y + xCO_2 \leftrightarrow 2xCO + \left(\frac{y}{2}\right)H_2$) promoted by CO_2, leading to an increase of H_2 and CO and decreasing CO_2 concentration in the gas [87]. This performance of producer gas composition aligns with biomass gasification results at 1000 °C with $O_2/CO_2/N_2$ medium [57,87].

The Steam-enhanced atmosphere evidenced for SCG a 21.30% relative content of H_2, presenting no significant improvement for H_2 production compared to O_2/N_2 medium. CH_4 presented a slight reduction from 8.09 to 7.40%. Meanwhile, the CO showed an increase from 35.77 to 44.32%. The results corroborate with Steam-enhanced gasification of SCG reported by [7]. However, unlike [7], which reported a CO_2 increase with the steam to biomass (S/B) molar ratio, the CO_2 decreased (from 34.85 to 26.98%). Therefore, the increase in H_2 and CO and decrease in CH_4 might be ascribed to the water gas reaction ($C + H_2O \rightarrow H_2 + CO$) and methane reforming ($CH_4 + H_2O \rightarrow CO + 3H_2$), promoted by steam medium [7]. Consequently, the H_2/CO molar ratio (Fig. 2(c)) of SCG increased (1%) for $O_2/CO_2/N_2$ and decreased (19.3%) for $O_2/H_2O/N_2$.

Fig. 2(b) evidenced an improved producer gas quality obtained by modifying the gasifying agent for BSG (increase of H_2 and CH_4 content). H_2 and CH_4 production increased significantly (up to 71.35 and 48.50%), with $O_2/N_2 < O_2/CO_2/N_2 < O_2/H_2O/N_2$. This behavior can be ascribed to the steam reforming of char and tar, as well as the water-gas shift reactions promoted by the steam and (indirectly) the CH_4-producing reactions [88,89].

Meanwhile, CO and CO_2 content for BSG presented the same trend, with $O_2/CO_2/N_2 < O_2/N_2 < O_2/H_2O/N_2$, where $O_2/H_2O/N_2$ presented higher values with an increase of 4.23% and 26.64% compared to O_2/N_2. Accordingly, comparing the O_2/N_2 with $O_2/CO_2/N_2$ gasification mediums, a decrease of 10.77% and 2.08% was evidenced for CO and CO_2. Therefore, the H_2/CO molar ratio of BSG gasification increased 33.52 and 64.39% for $O_2/CO_2/N_2$ and $O_2/H_2O/N_2$.

Fig. 2(c) presents H_2/CO ratios lower than 1 for both feedstocks. Therefore, the obtained syngas are suitable for synthesizing long-chain hydrocarbons, where lower H_2/CO values (between 0.25 and 0.9) are desired, and CO_2 is also required [57,90]. However, the lower H_2/CO limits the syngas' direct use in a Fischer-Tropsch process, which requires H_2/CO ratios between 2 and 3 [57,90].

The LHV_{syngas}, estimated by Equation (6), is intrinsically related to the producer gas composition. Fig. 2(c) show that for SCG, the LHV_{syngas} obtained with $O_2/CO_2/N_2$ and $O_2/H_2O/N_2$ medium, increased 3.09% and 7.73% compared to O_2/N_2. It can be seen that CO relative content has an important influence on this behavior since H_2 and CH_4 minimally varied (positive or negative) with gasification medium. The result is in line with [7], which evidenced higher LHV_{syngas} with increasing S/B and CO_2 concentration for SCG gasification.

A significant increase of LHV_{syngas} (up to 32.97%) was evidenced for BSG, following the same trend ($O_2/N_2 < O_2/CO_2/N_2 < O_2/H_2O/N_2$) as the H_2 and CH_4 relative content, corroborating with gasification of farms residues in the same reactor [57]. The calculated LHV_{syngas} values were 13.59, 13.92 and 18.07 $MJ.Nm^{-3}$ for O_2/N_2, $O_2/CO_2/N_2$ and $O_2/H_2O/N_2$, respectively.

The calculated CGE, CCE and γ_{syngas} (Fig. 2(d)) are functions of the syngas flow rate (Q_{syngas}), obtained experimentally. The results of Q_{syngas} for SCG (Table 3) were 0.075, 0.074 and 0.098 $Nm^3.h^{-1}$ for O_2/N_2, $O_2/CO_2/N_2$, and $O_2/H_2O/N_2$, respectively. For BSG, the experimental Q_{syngas} values were 0.026, 0.030, 0.037 $Nm^3.h^{-1}$ for O_2/N_2, $O_2/CO_2/N_2$, and $O_2/H_2O/N_2$, respectively.

Table 3

Syngas flow rate ($Nm^3.h^{-1}$), H_2 molar yields ($mol.kg_{biomass}^{-1}$), chemical and physical exergy values ($kJ.kg_{biomass}^{-1}$) of produced hydrogen and H_2 exergy efficiency (%).

	Q_{syngas} [a]	H_2 yield [b]	Ex^{ch}	Ex^{ph}	η_{H_2}
SCG ($\beta = 1.439$)					
O_2/N_2	0.0754	25.21	5952	410.30	20.57
$O_2/CO_2/N_2$	0.0745	25.82	6096	420.20	21.07
$O_2/H_2O/N_2$	0.0979	32.74	7730	532.80	26.72
BSG ($\beta = 1.783$)					
O_2/N_2	0.0260	12.52	2956	203.80	11.41
$O_2/CO_2/N_2$	0.0295	16.95	4002	275.90	15.44
$O_2/H_2O/N_2$	0.0374	30.87	7288	502.40	28.12

Fig. 2(d) evidence that the performance indicators (CGE, CCE and γ_{syngas}) had a similar trend for both biomasses, with higher values following the gasification mediums order $O_2/H_2O/N_2 > O_2/N_2 > O_2/CO_2/N_2$, which is consistent with producer gas composition and LHV_{syngas}. Although the SCG gasification presented a higher $\dot{m}_{bio}$ and carbon content (y_{carbon}) on its biomass feedstock compared to BSG, its CGE and CCE values were superior due to the higher Q_{syngas}. The CGE, CCE and γ_{syngas} varied between 122.28 and 170.97%, 141.07–189.03% and 91.97–129.54 $mol\ syngas.kg_{biomass}^{-1}$ for SCG and 94.76–181.27%, 80.8–136.22% and 27.90–67.52 $mol\ syngas.kg_{biomass}^{-1}$ for BSG, respectively. The obtained results align with SCG gasification results from [7] and other biomasses [57].

In this study, the exergy of produced H_2 (Fig. 3(a)) and the H_2 exergy efficiency (Fig. 3(b)) provide another performance indicator for gasification processes. Generally, exergy analysis is more meaningful and valuable than energy analysis, and it provides more insights into efficiency assessment [54,55]. Fig. 3

Fig. 3(a) and Table 3 show a higher total H_2 exergy for SCG than BSG for the Steam and CO_2-enhanced gasification mediums against conventional gasification, aligning with energy results. The results corroborate with gasification literature for SCG and are in the range of other common biomass residues [55,61]. The H_2 total exergy of CO_2-enhanced gasification increased by 2.42 and 35.39% for SCG and BSG compared to O_2/N_2, in line with [61] that reported an H_2 exergy increase with increasing CO_2/B ratio in gasification medium for different biomass feedstocks. Regarding Steam-enhanced gasification, the total exergy of H_2 production (Fig. 3(b)) increased 29.87 and 146.5% for SCG and BSG against conventional gasification.

Fremaux et al. (2015) investigated steam-enhanced gasification of wood residue at various S/Bs (0.5–1) for hydrogen production and reported an exergy efficiency increasing for higher S/Bs [91]. The increasing exergy of H_2 production might be attributed to the H_2 yields growths, which can be fundamentally associated with the fact that more moisture content at high gasification temperatures boosted the steam reforming reactions [55,92]. As expected, the resulted growth in the H_2 yield during Steam-enhanced gasification led to higher exergy of produced H_2 and consequently to a higher η_{H_2} for SCG and BSG (Table 3).

Fig. 3(b) presents the exergy efficiency of hydrogen production. The increase of the η_{H_2} followed the gasification order $O_2/N_2 < O_2/CO_2/N_2 < O_2/H_2O/N_2$, varying between 20.57 and 26.72% for SCG and 11.41 to 28.12% for BSG. Comparing SCG and BSG biomasses, the η_{H_2} was higher for SCG with O_2/N_2 and $O_2/CO_2/N_2$ gasification atmospheres. Contrarily, for $O_2/H_2O/N_2$, the η_{H_2} was higher for BSG. It can be seen from Table 3 that the H_2 yield and the chemical and physical exergy are similar for the Steam-enhanced gasification of SCG and BSG. Therefore the lower η_{H_2} of SCG with $O_2/H_2O/N_2$ conditions might be attributed to the lower $LHV_{biomass}$ of BSG compared to SCG. Results indicate that both biomasses reported encouraging H_2 exergy values and efficiency for green-hydrogen production.

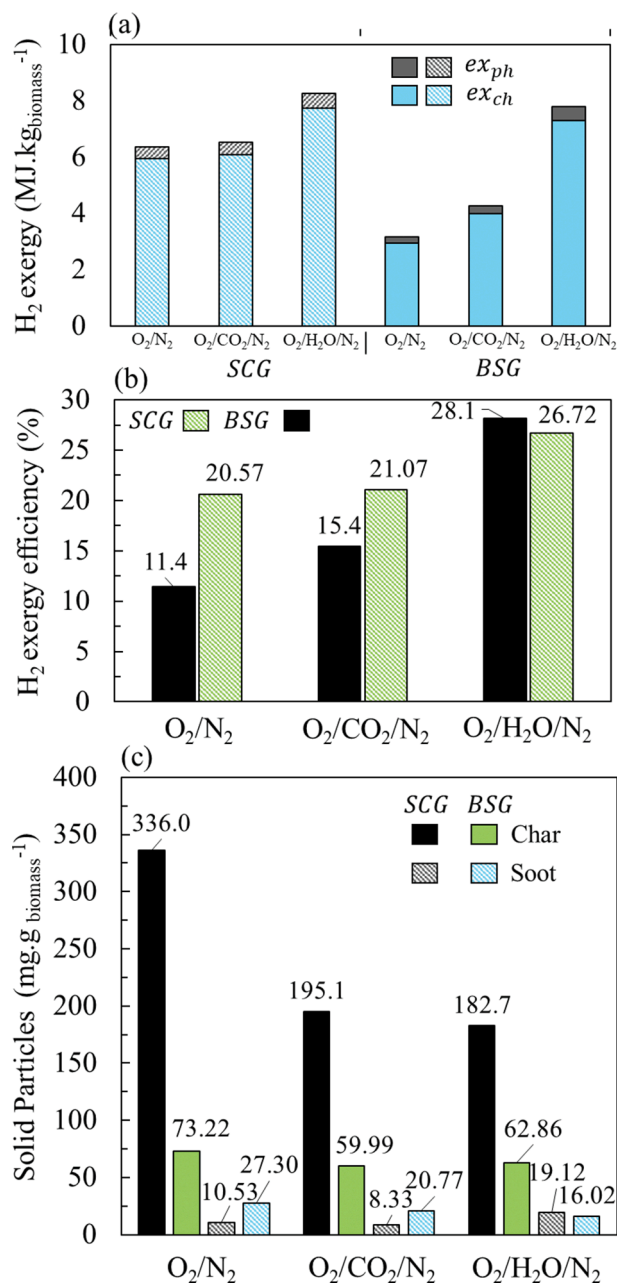Char and soot formed during the gasification experiments as a

Fig. 3. (a) Hydrogen exergy, (b) H_2 exergy efficiency (c) Soot and char formation for SCG and BSG gasification as a function of the gasification gas medium. (1-column fitting).

function of the gasification medium are presented in Fig. 3(c). The char formed during SCG gasification reduced for Steam/CO_2-enhanced gasification being $O_2/N_2 > O_2/CO_2/N_2 > O_2/H_2O/N_2$. The char yields were 336.01 mg.$g_{biomass}^{-1}$ (O_2/N_2), 195.13 mg.$g_{biomass}^{-1}$ for $O_2/CO_2/N_2$, and 182.65 mg.$g_{biomass}^{-1}$ for $O_2/H_2O/N_2$. The BSG gasification reported greater char yield values for O_2/N_2 with 73.22 mg.$g_{biomass}^{-1}$, followed by a decrease for $O_2/CO_2/N_2$ (59.99 mg.$g_{biomass}^{-1}$) and 62.86 mg. $g_{biomass}^{-1}$ for $O_2/H_2O/N_2$. The results are in line with steam gasification (1000–1400 °C) of beech sawdust in a DTR [93,94].

Concerning SCG gasification, soot formation presented 10.53, 8.33, and 19.12 mg.$g_{biomass}^{-1}$ for O_2/N_2, $O_2/CO_2/N_2$ and $O_2/H_2O/N_2$, respectively. For BSG, the soot formation was decreased with the Steam/ CO_2-enhanced gasification, with 27.30 mg.$g_{biomass}^{-1}$ for O_2/N_2 compared to 20.77 and 16.02 mg.$g_{biomass}^{-1}$ for $O_2/CO_2/N_2$ and $O_2/$ H_2O/N_2. The reduction of soot formation for BSG steam gasification

could be ascribed to an increase in soot oxidation or suppression of soot formation (due to OH) [57,94]. The results are in line with other biomasses showing that steam in the gasifying agent could promote the reforming of the tars and the soot reforming reaction, inhibiting the soot formation [57,58,93,94].

The CO_2 emission (E_{co_2}) results are presented in Table 4 for SCG and BSG. This performance indicator is related to the producer gas composition discussed previously and presented in Fig. 2(a and b). Considering the SCG, the E_{co_2} decreased from 0.61 (O_2/N_2) to 0.56 ($O_2/CO_2/N_2$) and 0.41 ($O_2/H_2O/N_2$). The BSG presented lower values when compared to the SCG. Equal E_{co_2} values of 0.2 were obtained for O_2/N_2 and $O_2/H_2O/$ N_2, and 0.19 for $O_2/CO_2/N_2$.

The multi-criteria decision analysis was used to evaluate the success rate of each biomass feedstock and gasification atmosphere considering the several performance indicators discussed here. Table 4 presents the obtained results for the SD, WD and d_n analyses. The last column (total success rate) is the average of the WD, SD, and d_n success rates [69]. The value expressed in the WD column represents how many other solutions have worse results than the one being analyzed [69]. Meanwhile, the SD values represent how many other solutions are inferior (considering all criteria) to the one being analyzed [69].

As can be seen, the same trend for the performance indicators was obtained for both low-cost biomass residues, aside from CCE and E_{co_2}. The $O_2/H_2O/N_2$ atmosphere provided the higher WD, SD, and d_n; therefore, the higher total success rate. For instance, the Steam-enhanced gasification (S/B = 0.5) characterizes the optimal operational condition within the considered indicators. Pondering SCG and BSG, the total success rates were 78% and 54% for $O_2/H_2O/N_2$, compared to 20% and 48% for $O_2/CO_2/N_2$ and 11% for conventional gasification (O_2/N_2) atmosphere.

Table 4

Producer gas results and its multi-criteria decision analysis.

	O_2/N_2	$O_2/CO_2/N_2$	$O_2/H_2O/N_2$
Spent coffee ground			
LHV_{syn}	10.45	10.77	11.26
CGE	122.28	124.42	170.97
CCE	141.07	139.45	189.03
γ_{syngas}	56.24	57.58	73.86
η_{H_2}	20.57	21.07	26.72
E_{CO_2}	0.61	0.56	0.41
S_D	1.00	1.00	2.00
W_D	0.00	0.00	2.00
d_n	0.20	0.15	0.00
S_D	33%	33%	67%
W_D	0%	0%	67%
d_n	0%	27%	100%
Total	11%	20%	78%
Brewing spent grain			
LHV_{syn}	13.59	13.92	18.07
CGE	94.76	110.24	181.27
CCE	80.83	87.33	136.22
γ_{syngas}	27.90	37.32	67.52
η_{H_2}	11.41	15.44	28.12
E_{CO_2}	0.20	0.19	0.20
S_D	1.00	2.00	2.00
W_D	0.00	1.00	0.00
d_n	0.05	0.03	0.00
S_D	33%	67%	67%
W_D	0%	33%	0%
d_n	0%	44%	94%
Total	11%	48%	54%

Pyrolysis

Pyrolysis products are evaluated as liquid (bio-oil), solid (biochar), and non-condensable (biogas) extents [95]. This work comprehensively investigates the biochar product as solid biofuel. Table 5 shows the biochar yields, its ultimate analysis and H/C and O/C molar ratios for the SCG and BSG.

The temperature effect on solid yield reduction is due to the devolatilization occasioned from the break of strong organic bonds of biomass organic matter [35]. The biochar yield reduced up to 72.74 and 73.02% for SCG and BSG. A noticeable decrease is evidenced between 300 and 500 °C treatments with a 28.44 and 20.88% reduction for SCG and BSG. This decrease can be ascribed principally to hemicelluloses and cellulose degradation [13,18]. The smoother reduction and the minor difference between biochar yields with increasing temperature (500–700 °C) might be attributed to the degradation of remaining lignin [51].

The difference between biochar yields in this temperature range was 1.5% for SCG and 1% for BSG. The SCG results align with [1] that reported 28.73 and 27.28% biochar yields for 500 and 700 °C pyrolysis experiments. Concerning the BSG, the results agree with [35] that show biochar yields of 27.96 and 26.11% for 450 and 650 °C pyrolyzes. Fig. 4 illustrates the H/C and O/C molar ratios (Table 5) in the Van Krevelen diagram for raw and obtained biochar of SCG and BSG.

The raw SCG and BSG presented a H/C of 1.67, 1.85 and O/C of 0.56, 0.76, in line with literature for SCG [4] and BSG [30,35]. It can be seen from Fig. 4 that during pyrolysis, H and O are released, and the aromaticity (H/C) and polarity (O/C) decrease with increases in the reaction temperature, converting it into a more coal-like fuel [35].

The pyrolysis temperature effect can be observed with the increasing carbon content of the biochar and the parallel decrease in the oxygen and hydrogen because of the decarboxylation and dehydration of biomass [35]. The H/C and O/C ratios indicate the degree of biochar reactivity to the different gases present in the combustion systems [96]. The low ratios obtained for biochar evidence a more aromatic and carbonaceous composition, releasing less water vapor and smoke than raw feedstock during combustion [35,96].

The CEI, which were calculated as a function of the biochar carbon content, are presented in Fig. 5(a and b) for SCG and BSG, providing a performance indicator for pyrolysis. A higher CEI is desired when applying biochar as biofuel. For instance, the results showed a linear increase as the pyrolysis temperatures grew, and the CEI values were 0.36, 0.57 and 1 for SCG and 0.51, 0.75 and 1 for BSG considering 300, 500 and 700 °C treatment, respectively.

The HHV value is closely related to the CEI and the atomic ratios of O/C and H/C [56]. As presented in Fig. 5(a), the calculated HHV of SCG increased for obtained biochars with 300 and 700 °C pyrolyzes. However, the 500 °C biochar presented lower HHV than biochar obtained at 300 °C and is similar to raw SCG. This behavior on HHV of 500 °C biochar might be attributed to the higher decrease of H content (67.04%) and a minor increase of C (28.30%) in comparison to raw SCG induced by a higher loss of organic liquids (coffee oils) related to
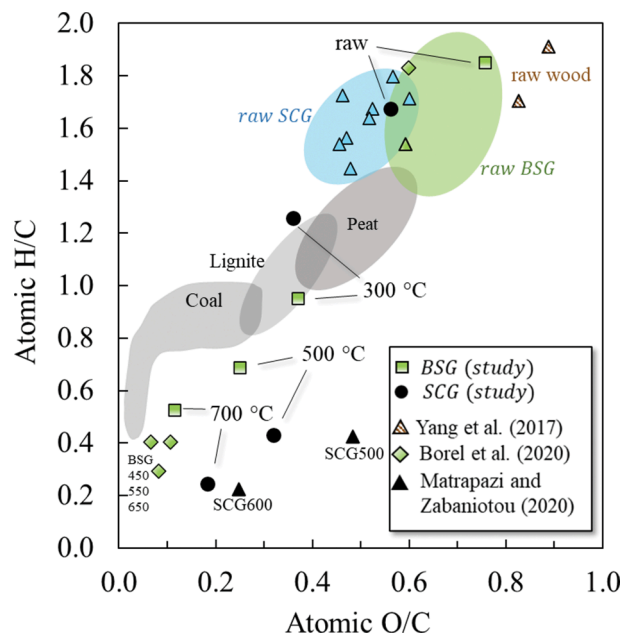

Fig. 4. Ultimate analysis for feedstock and pyrolyzed products (a) SCG and (b) BSG. (c) Van Krevelen diagram. Data of raw SCG from ([4]) and BSG from ([30]) (1-column fitting).

extractible contents [97].

The increase of the HHV, evaluated by its EF, varied between 17.5 and 19.42 MJ.kg^{-1} for SCG. On the other hand, the HHV of BSG (Fig. 5 (b)) presented a notorious linear increase (EF up to 83.11%) as the pyrolysis temperature increased, varying between 17.06 and 31.23 MJ. kg^{-1}. Results corroborate with elemental composition modification in the obtained biochar (Table 5) and BSG pyrolysis results reported by [30].

The solid fuel upgrading from pyrolysis aims to obtain biochar with high energy yield at a low solid volume to increase the processing efficiency and simplify handling, transportation, and logistics [76], and the EMCI provides the required information for this evaluation. For example, Fig. 5(c) shows that 300 °C and 700 °C provided interesting results concerning energy densification (higher EY than BY) with EMCI of 9.79 and 5.29. However, the 500 °C evidenced a negative result with an EMCI of −0.16, not optimizing the energy density of the obtained biochar.

Meanwhile, all performed pyrolysis were beneficial for BSG concerning energy densification (Fig. 5(d)), with the optimal condition at 700 °C, followed by 300 °C and 500 °C with EMCI values of 22.42, 17.33 and 14.58, respectively. Thus, comparing both biomasses EMCI, BSG presented higher values as optimized solid biofuel. The worst condition was obtained at 500 °C for both biomasses with optimized biochar at 300 °C for SCG and 700 °C for BSG.

The surface morphological modifications caused by SCG and BSG

Table 5
Biochar yield (SY) and ultimate analysis (wt%) results for different pyrolysis temperatures considering SCG and BSG.

| Temperature	BY	C	H	O	N	H/C	O/C	Formula
SCG								
raw	100.00	51.74	7.22	38.65	2.39	1.66	0.56	$CH_{1.66}O_{0.56}$
300 °C	55.70	61.06	6.40	29.21	3.33	1.25	0.36	$CH_{1.25}O_{0.36}$
500 °C	28.79	66.38	2.38	28.16	3.08	0.43	0.32	$CH_{0.43}O_{0.32}$
700 °C	27.26	77.29	1.57	18.85	2.29	0.24	0.18	$CH_{0.24}O_{0.18}$
BSG								
raw	100.00	44.72	6.86	44.66	3.21	1.83	0.75	$CH_{1.83}O_{0.75}$
300 °C	48.84	63.28	5.03	31.20	0.49	0.95	0.37	$CH_{0.95}O_{0.37}$
500 °C	27.96	71.67	4.11	23.84	0.38	0.68	0.25	$CH_{0.68}O_{0.25}$
700 °C	26.98	83.17	3.66	12.62	0.55	0.52	0.11	$CH_{0.52}O_{0.11}$
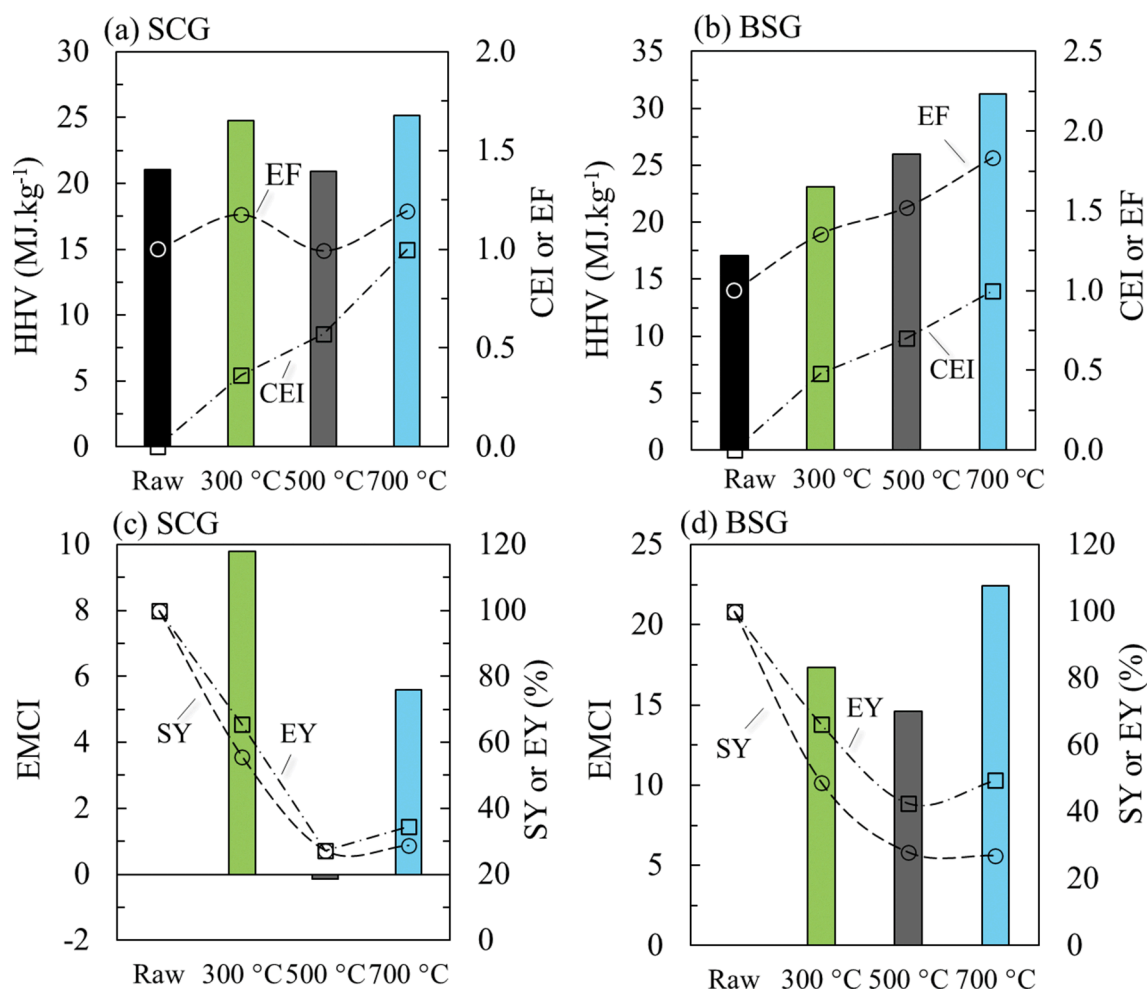
Fig. 5. (a) HHV, (b) EF, (c) MY, EY and EMCI, (d) CEI of the pyrolyzed biochar for SCG and BSG as a function of temperature treatment. (2-column fitting).

pyrolysis can be observed by comparing the SEM images of the raw materials and the biochar particles for 300, 500 and 700 °C treatments. The SEM images for SCG and SCG-biochar are shown in Fig. 6(a–h) at magnifications of 400X and 1000X for raw, 300, 500 and 700 °C, respectively.

The SCG raw material surface consists mainly of flakes presenting uneven lumps of different sizes with shallow pores. After pyrolysis treatment, minor differences are observed on the biochar surfaces with higher treatment severities. As a result, the surfaces of SCG presented a more vivid porous-like structure, in line with [1,7]. This char characteristic might be helpful in other applications as absorption of a wide range of contaminants (heavy metals) in the water cleaning process, energy storage application (electrode), fabrication of humidity sensor [98].

Considering the BSG, Fig. 6(e) shows that the surface of the biochar is amorphous and heterogeneous, with microporous and fibrous texture regions, in line with [35]. Machado et al. (2020) and Fontana et al. (2018) reported that the morphology of the vegetative tissue of raw malt bagasse formed a kind of fibers overlapping, presenting a rigid structure with irregularities, which probably composes the vascular system of the plant [36,99], in line with Fig. 6(e).

Through Fig. 6(f–h), it was possible to observe the effect of pyrolysis on the biochar surface. The magnification of 1000X provided details of some cavities in the plant wall, which are characteristic of plant structures [36]. For higher temperatures, the opening of these cavities can be evidenced. This observation might be attributed to the fast volatile release at high temperatures (700 °C), leading to an internal over-pressure [100]. According to the performed analysis, the results reveal

that the pyrolysis process significantly impacts the SCG and BSG biochar chemically rather than on its physical characteristics, agreeing with SEM results for SCG and BSG [1,35].

The multi-criteria decision analysis was conducted for a comprehensive and extended assessment of SCG and BSG biochars. Table 6 presents the evolved performance parameters and the results for the S_d, W_d and d_n methods. The optimal operational condition is attained for the higher total success rate contemplating each decision method [69].

As can be seen, both biomasses obtained the optimal performance at 700 °C, due to lower H/C and O/C ratios, higher HHV and EF. The EY is a critical performance parameter to be considered in the DA because it accounts for the BY reduction promoted by pyrolysis (in contrast to the higher desired BY for a more significant amount of biochar).

As discussed later, a lower EY for 500 °C SCG and BSG was evidenced, indicating the worst EMCI for both biomasses in this temperature. Throughout the DA, the lower EY pondered the S_d, W_d and d_n in a way that 300 and 500 °C pyrolyzes had similar (BSG) or intermediate (SCG) success rates. Regarding all the evolved performance indicators, the SCG and BSG showed that 700>300>500 °C, with a minor difference between 300 and 500 °C, corroborating the EMCI results.

This work focused on solid biofuel (biochar) production via pyrolysis. It is well known that the pyrolysis process's operation conditions are essential in defining pyrolytic products yields and providing different physicochemical properties for respective products. Future studies may include using multi-parameter analysis further to investigate bio-oil and pyro-gas production for different applications.
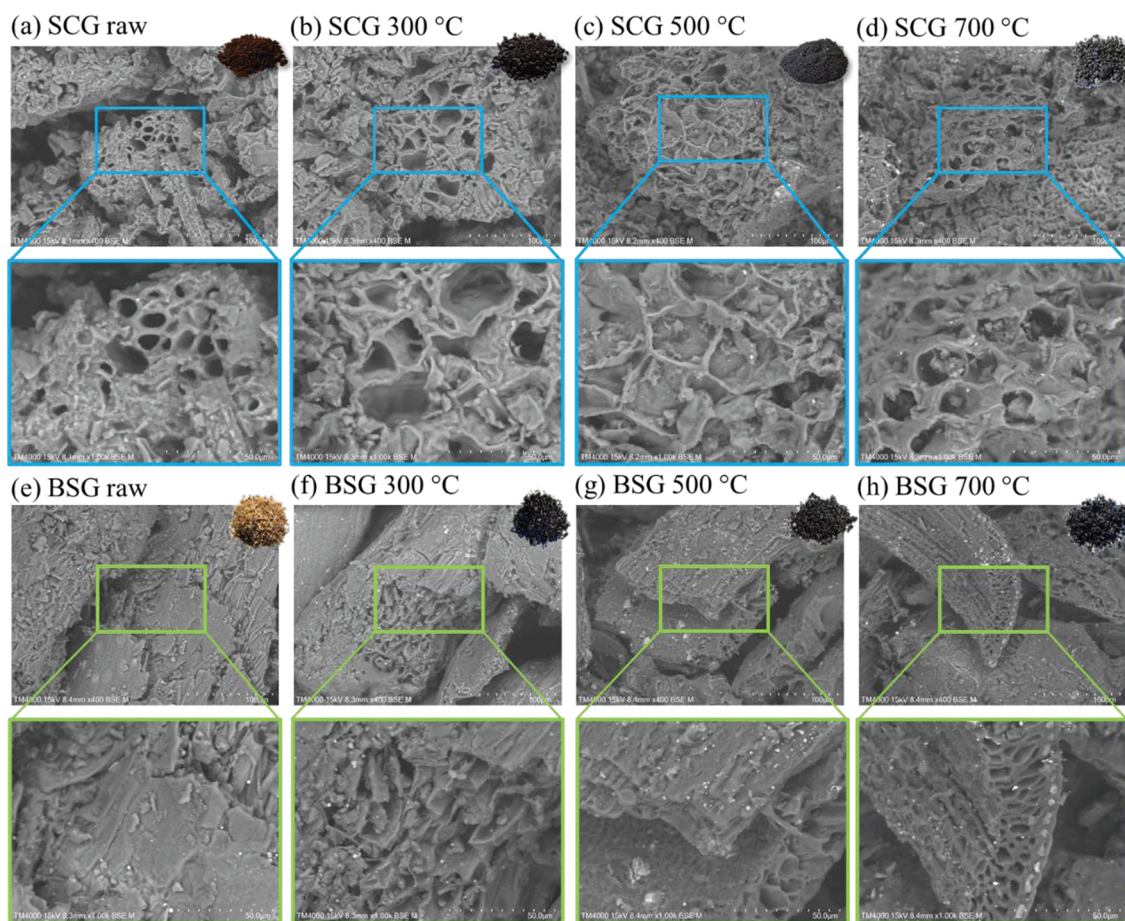
Fig. 6. SCG SEM images with 400 and 1000X for Raw (a), 300 °C (c), 500 °C (b), and 700 °C(d). BSG SEM images with 400 and 1000X for Raw (e), 300 °C (f), 500 °C (g), and 700 °C (h). (2-column fitting).

Table 6
Energy performance indicators for the SCG and BSG biochar and its multi-criteria decision analysis for biofuel application.

(°C)	H/C	O/C	HHV	EF	EY	S_D	W_D	d_n	S_D	W_D	d_n	Total
Spent coffee ground (SCG)												
raw	1.66	0.56	21.04	1.00	100	3	0	1.42	75%	0%	0%	25%
300	1.25	0.36	24.73	1.18	65.49	3	0	1.01	75%	0%	29%	35%
500	0.43	0.32	20.92	0.99	28.63	2	0	0.69	50%	0%	52%	34%
700	0.24	0.18	25.12	1.19	32.55	3	1	0.02	75%	25%	99%	66%
Brewing spent grain (BSG)												
raw	1.83	0.75	17.06	1.00	100	3	0	1.32	75%	0%	0%	25%
300	0.95	0.37	23.11	1.35	66.10	3	0	0.43	75%	0%	67%	47%
500	0.68	0.25	25.95	1.52	42.50	2	0	0.18	50%	0%	87%	46%
700	0.52	0.11	31.23	1.83	49.35	3	1	0.01	75%	33%	99%	69%

Combustion behavior

The TG, DTG curves for SCG and BSG, as well as the two-dimensional TG mapping with the combustion temperatures, are presented in Fig. 7 (a–f), respectively for SCG and BSG. In addition, the characteristic combustion parameters of the SCG and BSG biochar are listed in Table 7. Determining these performance indicators for combustion requires the characteristic parameters reflecting thermal behavior during the combustion process [101]. The T_i, T_p, T_f, D_i, D_f and S can be obtained from the analysis of combustion TG and DTG curves [84,102,103], which allows a quantitative comparison of the combustion characteristics of SCG and BSG biochars.

Fig. 7 shows that thermal stability increases after the drying phase as the pyrolysis temperature increases for SCG and BSG. Therefore, the TG

and DTG profiles shift for the regions of high temperatures, in line with biochar of babassu coconut combustion [104] and semicokes derived from pyrolysis of low-rank bituminous coal [105]. Consequently, the T_p (Fig. 7(e and f)) were smaller for raw SCG and BSG with 312.55 and 299.22 °C compared to biochar's. The SCG and BSG presented closer T_p for 300 and 500 °C treatments, differing by $\approx$ 4 °C. Regarding 700 °C treatment, the T_p decreased for SCG and increased for BSG compared to 500 °C.

As can be seen in Fig. 7 and Table 7, the raw material showed more reactivity in the initial phase of combustion, presenting a T_i of 274.48 °C and 256.06 °C for SCG and BSG, respectively. Results are in line with other biomass residues [103,104], describing relatively low temperatures than charcoal [105] due to the higher volatile matter/fixed carbon ratio in the solid fuel [104]. The burnout temperature (T_f) of raw
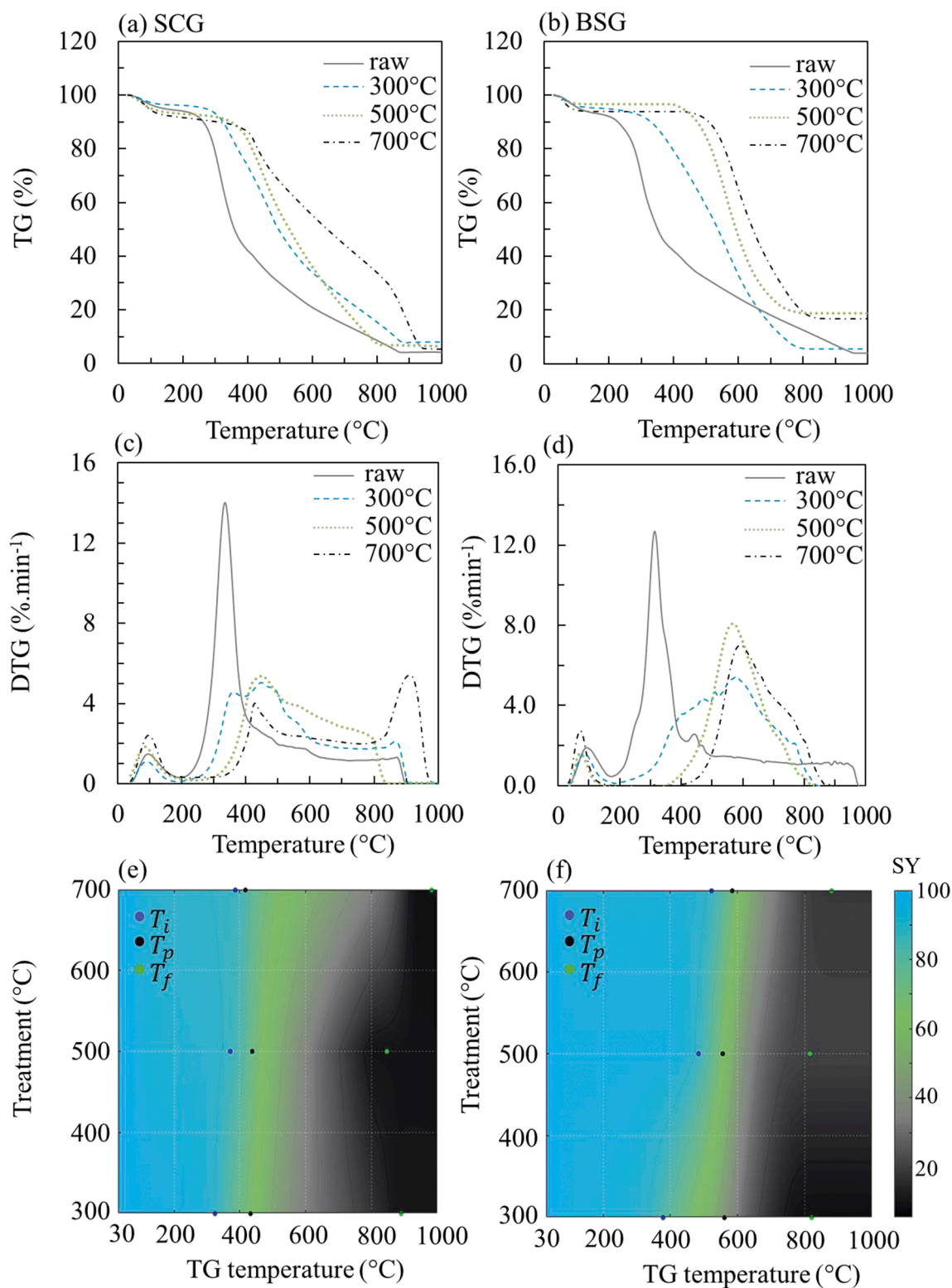
Fig. 7. TG (a)(b), DTG (c)(d) and TG contour mapping (e)(f) of SCG and BSG for 300, 500 and 700 °C. (2-column fitting).

material was 872.92 °C and 956.83 °C for SCG and BSG. The obtained T_f were higher than other raw biomass residues [103,104]. Wnorowska et al. (2020) investigated different fuel types and showed that the burnout temperature was higher when higher heating rates were applied. Therefore, the higher T_f obtained for SCG and BSG might be attributed to the 33 °C.min^{-1} applied in comparison to 1.67 °C.min^{-1} for babassu coconut [104] and (5, 10, 15 and 20 °C.min^{-1}) for herbaceous

and cereal straw biomasses [103].

The D_i denotes the ignition capacity of fuel so that the higher D_i, the more volatile compounds are separated from fuel, the easier the fuel ignition occurs [81,82]. The D_f denotes the combustion capacity of a fuel [81]. Table 7 shows that the ignition index D_i of SCG and BSG biochar were lower than raw material. The D_i and D_f remained almost unchanged when pyrolysis temperature was 300 and 500 °C, but both

Table 7
Combustion characteristic parameters of SCG and BSG.

SCG	T_i (°C)	T_p (°C)	T_f (°C)	$D_i \times 10^3$	$D_f \times 10^4$	$S \times 10^6$
Raw	274.48	312.55	874.43	1.52	34.34	9.08
300 °C	325.34	432.72	890.82	0.32	4.84	2.13
500 °C	371.37	437.46	845.84	0.30	4.46	1.87
700 °C	386.15	417.70	982.73	0.24	3.07	1.14
BSG						
Raw	256.06	299.22	962.52	89.88	18.32	8.34
300 °C	378.35	560.85	820.08	12.33	3.47	1.86
500 °C	482.95	556.59	816.97	14.60	3.75	1.47
700 °C	521.63	585.09	880.40	10.99	2.60	1.04

D_i (%.min^{-3}), D_f (%.min^{-4}) and S (%$^{-2}$.min^{-2}.°C^{-3}).

indexes decreased for 700 °C pyrolysis, agreeing with [104,105]. In other words, the biochar obtained at higher pyrolysis temperatures presented inferior ignition performance, which is harder to ignite, and the burnout efficiency is lower, in line with [105]. This behavior might be attributed to the faster releasing and the greatest amount of volatile materials within raw biomass and obtained biochar at lower pyrolysis severities contributing decisively to accelerate the fuel ignition at a lower temperature [106]. Regarding BSG, it is important to note that D_i and D_f increased a small percentage of 1.46 and 8.06% for 500 °C compared to 300 °C, showing better ignition performance and burnout efficiency.

The characteristic combustion index (S) reflects the reactivity of biochar combustion throughout the oxidation reaction [83,104,105]. SCG and BSG presented a similar range for S and linear decreased as the pyrolysis temperature increases with 23.5 and 22.3% for 300 °C, 20.6, 17.6% for 500 °C and 12.5% for 700 °C. Results are in line with carbonization for bamboo sawdust and cotton stalk [101] and babassu nutshell [104]. Therefore, the obtained biochars at lower temperatures are easier to ignite and have better combustibility, burning more quickly and powerfully [101,104].

The obtained combustion index for SCG and BSG are considerably higher than those obtained by Protásio et al. (2017) for babassu nutshell pyrolysis (450–850 °C) and Qian et al. (2012) for pyrolyzed low-rank coal (450–650 °C) that reported S values ranging between 4.93×10^{-7}–1.56×10^{-7} and 1.24×10^{-7}–9.40×10^{-8} %^{2}.min^{-2}.°C^{-3}. As a result, the compared S values indicated the great potential of using SCG and BSG as solid biofuel for straightforward application to heat generation in small-scale systems.

Conclusion

This work comprehensively investigated steam/CO_2-enhanced gasification and pyrolysis processes for the low-cost and constantly supplied SCG and BSG residues. The multi-parameter decision analysis allowed identifying and comparing optimal operational conditions for the gasification and pyrolysis parameters.

SCG gasification evidenced high LHV_{syngas} with increasing S/B and CO_2 concentration gasification. A significant increase of H_2 and CH_4 relative content, consequently LHV_{syngas} (up to 32.97%) was evidenced for BSG. Therefore, the performance indicators (CGE, CCE and γ_{syngas}) had a similar trend for both biomasses, with higher values following the gasification mediums order $O_2/H_2O/N_2 > O_2/N_2 > O_2/CO_2/N_2$.

Steam-enhanced gasification promoted the increase of H_2 relative yield during gasification boosting the exergy of produced green hydrogen and, consequently the η_{H_2} for SCG and BSG. The multi-parameter analysis revealed that the Steam-enhanced gasification (S/B = 0.5) provided the higher WD, SD, and d_n; therefore, the higher total success rate of 78% and 54% for SCG and BSG, characterizing the optimal operational condition within the considered indicators.

The produced biochar reported reduced H/C and O/C, promoting an HHV enhancement of 19.42% (SCG) and 83.11% (BSG). Decision

analysis results showed that $700 > 300 > 500$ °C, with minor differences between 300 and 500 °C, in line with the energy-mass co-benefit index analysis. Moreover, pyrolysis significantly impacts the SCG and BSG biochar chemically rather than on its physical characteristics.

The TGA allowed identifying higher ignitions temperatures and burnout indexes and lower ignition indexes for biochar produced at lower pyrolysis temperatures, which characterizes better ignitability and combustibility, burning more quickly and powerfully. The S values indicated a great potential of using SCG and BSG as solid biofuel for straightforward application to heat generation in small-scale systems compared to other biomass residues.

The perceptive conclusions of this paper could support in recommending optimum paths to more economically valorization of low-cost feedstock through pyrolysis and gasification valorization route, encouraging waste-to-energy development and circular economy principles.

CRediT authorship contribution statement

Rafael B.W. Evaristo: Formal analysis, Investigation, Writing – review & editing. **Ricardo Ferreira:** Formal analysis, Investigation, Writing – review & editing. **Juliana Petrocchi Rodrigues:** Formal analysis, Investigation, Writing – review & editing. **Juliana Sabino Rodrigues:** Investigation, Writing – review & editing. **Grace F. Ghesti:** Conceptualization, Funding acquisition, Investigation, Project administration, Writing – original draft, Writing – review & editing. **Edgar A. Silveira:** Conceptualization, Formal analysis, Writing – original draft. **M. Costa:** Conceptualization, Methodology, Resources, Supervision.

Declaration of Competing Interest

The authors declare that they have no known competing financial interests or personal relationships that could have appeared to influence the work reported in this paper.

Appendix A. Supplementary data

Supplementary data to this article can be found online at https://doi.org/10.1016/j.ecmx.2021.100138.

References

[1] Lee XJ, Ong HC, Gao W, Ok YS, Chen W-H, Goh BHH, et al. Solid biofuel production from spent coffee ground wastes: Process optimisation, characterisation and kinetic studies. Fuel 2021;292:120309. https://doi.org/10.1016/j.fuel.2021.120309.
[2] Cséfalvay E, Horváth IT. Sustainability Assessment of Renewable Energy in the United States, Canada, the European Union, China, and the Russian Federation. ACS Sustain Chem Eng 2018;6(7):8868–74. https://doi.org/10.1021/acssuschemeng.8b0121310.1021/acssuschemeng.8b01213.s001.

[3] Dhillon RS, von Wuehlisch G. Mitigation of global warming through renewable biomass. Biomass Bioenergy 2013;48:75–89. https://doi.org/10.1016/j. biombioe.2012.11.005.

[4] Atabani AE, Ali I, Naqvi SR, Badruddin IA, Aslam M, Mahmoud E, et al. A state-of-the-art review on spent coffee ground (SCG) pyrolysis for future biorefinery. Chemosphere 2022;286:131730. https://doi.org/10.1016/j. chemosphere.2021.131730.

[5] Zabaniotou A, Kamaterou P. Food waste valorization advocating Circular Bioeconomy – A critical review of potentialities and perspectives of spent coffee grounds biorefinery. J Clean Prod 2019;211:1553–66. https://doi.org/10.1016/j. jclepro.2018.11.230.

[6] Murthy PS, Madhava NM. Sustainable management of coffee industry by-products and value addition – A review. Resour Conserv Recycl 2012;66:45–58. https://doi.org/10.1016/j.resconrec.2012.06.005.

[7] Kibret HA, Kuo YL, Ke TY, Tseng YH. Gasification of spent coffee grounds in a semi-fluidized bed reactor using steam and CO2 gasification medium. J Taiwan Inst Chem Eng 2021;119:115–27. https://doi.org/10.1016/j.jtice.2021.01.029.

[8] Cenci IdO, Guimarães BP, Amabile RF, Ghesti GF. Comparison between barley malt protein quantification methods. Food. Sci Technol 2021;41(suppl 1):213–7. https://doi.org/10.1590/fst.13920.

[9] Lima LA, Fernandes TL, Tenório LXdS, Silva MLd, Evaristo RBW, Ghesti GF, et al. Sinopse Do Cenário Cervejeiro: O Advento Da Produção E O Mercado Na Região Centro Oeste. Cad Prospecção 2017;10:650.;10(4):650. https://doi.org/10.9771/cp.v10i4.23041.

[10] Olajire AA. The brewing industry and environmental challenges. J Clean Prod 2020;256:102817. https://doi.org/10.1016/j.jclepro.2012.03.003.

[11] Mussatto SI, Dragone G, Roberto IC. Brewers' spent grain: generation, characteristics and potential applications. J Cereal Sci 2006;43(1):1–14. https://doi.org/10.1016/j.jcs.2005.06.001.

[12] Costa T da S, Caldeira-Pires A, Silveira EA, Cardoso AN, Kovaleski S, Gouvea JA de. Environmental impact analysis of brazil's southern region canola oil production. 29th Eur. Biomass Conf. Exhib., 2021, p. 1168–71. https://doi.org/10.5071/29thEUBCE2021-4AV.3.14.

[13] Ortiz I, Torreiro Y, Molina G, Maroño M, Sánchez JM. A Feasible Application of Circular Economy: Spent Grain Energy Recovery in the Beer Industry. Waste Biomass Valorization 2019;10(12):3809–19. https://doi.org/10.1007/s12649-019-00677-y.

[14] Santanna MS, Silveira EA, Caldeira-Pires A. Thermochemical pathways for municipal lignocellulosic waste as biofuel. 29th Eur. Biomass Conf. Exhib. 2021. https://doi.org/10.5071/29thEUBCE2021-3DV.6.8.

[15] Chaves BS, Macedo LA, Galvão LGO, Carvalho ACR, Palhano AX, Vale AT, et al. Production and characterization of raw and torrefied phyllostachys aurea pellets and briquettes for energy purposes. 29th Eur. Biomass Conf. Exhib. 2021:657–61. https://doi.org/10.5071/29thEUBCE2021-2DV.2.1.

[16] Silveira Edgar A, Luz Sandra M, Leão Rosineide M, Rousset Patrick, Caldeira-Pires Armando. Numerical modeling and experimental assessment of sustainable woody biomass torrefaction via coupled TG-FTIR. Biomass Bioenergy 2021;146: 105981. https://doi.org/10.1016/j.biombioe.2021.105981.

[17] You Siming, Ok Yong Sik, Chen Season S, Tsang Daniel CW, Kwon Eilhann E, Lee Jechan, et al. A critical review on sustainable biochar system through gasification: Energy and environmental applications. Bioresour Technol 2017; 246:242–53. https://doi.org/10.1016/j.biortech.2017.06.177.

[18] Xiu Shuangning, Shahbazi Abolghasem, Wallace Carlington W, Wang Lijun, Cheng Dan. Enhanced bio-oil production from swine manure co-liquefaction with crude glycerol. Energy Convers Manag 2011;52(2):1004–9. https://doi.org/10.1016/j.enconman.2010.08.028.

[19] Ong Hwai Chyuan, Chen Wei-Hsin, Singh Yashvir, Gan Yong Yang, Chen Chia-Yang, Show Pau Loke. A state-of-the-art review on thermochemical conversion of biomass for biofuel production: A TG-FTIR approach. Energy Convers Manag 2020;209:112634. https://doi.org/10.1016/j.enconman.2020.112634.

[20] Silveira EA, Luz S, Santanna MS, Leão RM, Rousset P, Pires AC. Thermal upgrading of sustainable woody material: experimental and numerical torrefaction assessment. 28th Eur. Biomass Conf. Exhib., Virtual 2020:694–8. https://doi.org/10.5071/28thEUBCE2020-3CV.2.5.

[21] Lin Bo-Jhih, Silveira Edgar A, Colin Baptiste, Chen Wei-Hsin, Pétrissans Anélie, Rousset Patrick, et al. Prediction of higher heating values (HHVs) and energy yield during torrefaction via kinetics. Energy Procedia 2019;158:111–6. https://doi.org/10.1016/j.egypro.2019.01.054.

[22] Silveira Edgar A, Luz Sandra, Candelier Kevin, Macedo Lucélia A, Rousset Patrick. An assessment of biomass torrefaction severity indexes. Fuel 2021;288:119631. https://doi.org/10.1016/j.fuel.2020.119631.

[23] Silveira Edgar A, Macedo Lucélia A, Candelier Kevin, Rousset Patrick, Commandré Jean-Michel. Assessment of catalytic torrefaction promoted by biomass potassium impregnation through performance indexes. Fuel 2021;304: 121353. https://doi.org/10.1016/j.fuel.2021.121353.

[24] Tsai WT, Liu SC, Hsieh CH. Preparation and fuel properties of biochars from the pyrolysis of exhausted coffee residue. J Anal Appl Pyrolysis 2012;93:63–7. https://doi.org/10.1016/j.jaap.2011.09.010.

[25] Vardon Derek R, Moser Bryan R, Zheng Wei, Witkin Katie, Evangelista Roque L, Strathmann Timothy J, et al. Complete utilization of spent coffee grounds to produce biodiesel, bio-oil, and biochar. ACS Sustain Chem Eng 2013;1(10): 1286–94. https://doi.org/10.1021/sc400145w.

[26] Li X, Strezov V, Kan T. Energy recovery potential analysis of spent coffee grounds pyrolysis products. J Anal Appl Pyrolysis 2014;110:79–87. https://doi.org/10.1016/j.jaap.2014.08.012.

[27] Matrapazi VK, Zabaniotou A. Experimental and feasibility study of spent coffee grounds upscaling via pyrolysis towards proposing an eco-social innovation circular economy solution. Sci Total Environ 2020;718:137316. https://doi.org/10.1016/j.scitotenv.2020.137316.

[28] Karmee SK. A spent coffee grounds based biorefinery for the production of biofuels, biopolymers, antioxidants and biocomposites. Waste Manag 2018;72: 240–54. https://doi.org/10.1016/j.wasman.2017.10.042.

[29] Mussatto Solange I. Brewer's spent grain: A valuable feedstock for industrial applications. J Sci Food Agric 2014;94(7):1264–75. https://doi.org/10.1002/jsfa.6486.

[30] Sanna Aimaro, Li Sujing, Linforth Rob, Smart Katherine A, Andrésen John M. Bio-oil and bio-char from low temperature pyrolysis of spent grains using activated alumina. Bioresour Technol 2011;102(22):10695–703. https://doi.org/10.1016/j.biortech.2011.08.092.

[31] Balogun AO, Sotoudehniakarani F, McDonald AG. Thermo-kinetic, spectroscopic study of brewer's spent grains and characterisation of their pyrolysis products. J Anal Appl Pyrolysis 2017;127:8–16. https://doi.org/10.1016/j.jaap.2017.09.009.

[32] Mahmood ASN, Brammer JG, Hornung A, Steele A, Poulston S. The intermediate pyrolysis and catalytic steam reforming of Brewers spent grain. J Anal Appl Pyrolysis 2013;103:328–42. https://doi.org/10.1016/j.jaap.2012.09.009.

[33] Vanreppelen Kenny, Vanderheyden Sara, Kuppens Tom, Schreurs Sonja, Yperman Jan, Carleer Robert. Activated carbon from pyrolysis of brewer's spent grain: Production and adsorption properties. Waste Manag Res 2014;32(7): 634–45. https://doi.org/10.1177/0734242X14538306.

[34] Borel LDMS, Lira TS, Ribeiro JA, Ataíde CH, Barrozo MAS. Pyrolysis of brewer's spent grain: Kinetic study and products identification. Ind Crops Prod 2018;121: 388–95. https://doi.org/10.1016/j.indcrop.2018.05.051.

[35] Borel Lidja DMS, Reis Filho Argileu M, Xavier Thiago P, Lira Taisa S, Barrozo Marcos AS. An investigation on the pyrolysis of the main residue of the brewing industry. Biomass Bioenergy 2020;140:105698. https://doi.org/10.1016/j.biombioe.2020.105698.

[36] Machado Lauren MM, Lütke Sabrina F, Perondi Daniele, Godinho Marcelo, Oliveira Marcos LS, Collazzo Gabriela C, et al. Simultaneous production of mesoporous biochar and palmitic acid by pyrolysis of brewing industry wastes. Waste Manag 2020;113:96–104. https://doi.org/10.1016/j.wasman.2020.05.038.

[37] Jung Sungyup, Shetti Nagaraj P, Reddy Kakarla Raghava, Nadagouda Mallikarjuna N, Park Young-Kwon, Aminabhavi Tejraj M, et al. Synthesis of different biofuels from livestock waste materials and their potential as sustainable feedstocks – A review. Energy Convers Manag 2021;236:114038. https://doi.org/10.1016/j.enconman.2021.114038.

[38] Ferreira S, Monteiro E, Calado L, Silva V, Brito P, Vilarinho C. Experimental and modeling analysis of brewers' spent grains gasification in a downdraft reactor. Energies 2019;12:1–18. https://doi.org/10.3390/en12234413.

[39] Parascanu MM, Sandoval-Salas F, Soreanu G, Valverde JL, Sanchez-Silva L. Valorization of Mexican biomasses through pyrolysis, combustion and gasification processes. Renew Sustain Energy Rev 2017;71:509–22. https://doi.org/10.1016/j.rser.2016.12.079.

[40] Torres C, Urvina L, de Lasa H. A chemical equilibrium model for biomass gasification. Application to Costa Rican coffee pulp transformation unit. Biomass Bioenergy 2019;123:89–103. https://doi.org/10.1016/j.biombioe.2019.01.025.

[41] Ismail TM, Abd El-Salam M, Monteiro E, Rouboa A. Eulerian – Eulerian CFD model on fluidized bed gasifier using coffee husks as fuel. Appl Therm Eng 2016; 106:1391–402. https://doi.org/10.1016/j.applthermaleng.2016.06.102.

[42] George Joel, Arun P, Muraleedharan C. Experimental investigation on co-gasification of coffee husk and sawdust in a bubbling fluidised bed gasifier. J Energy Inst 2019;92(6):1977–86. https://doi.org/10.1016/j.joei.2018.10.014.

[43] Couto N, Silva V, Monteiro E, Brito PSD, Rouboa A. Experimental and numerical analysis of coffee husks biomass gasification in a fluidized bed reactor. Energy Procedia 2013;36:591–5. https://doi.org/10.1016/j.egypro.2013.07.067.

[44] de Oliveira Jofran Luiz, da Silva Jadir Nogueira, Martins Marcio Arêdes, Pereira Emanuele Graciosa, da Conceição Trindade Bezerra e Oliveira Maria. da Conceição Trindade Bezerra e Oliveira M. Gasification of waste from coffee and eucalyptus production as an alternative source of bioenergy in Brazil. Sustain Energy Technol Assessments 2018;27:159–66. https://doi.org/10.1016/j.seta.2018.04.005.

[45] Pacioni TR, Soares D, Di Domenico M, Rosa MF, de Moreira FPM R, José HJ. Bio-syngas production from agro-industrial biomass residues by steam gasification. Waste Manag 2016;58:221–9. https://doi.org/10.1016/j.wasman.2016.08.021.

[46] Pacioni TR, Soares D, Di Domenico M, Alves JLF, Virmond E, de Moreira R, et al. Kinetic modeling of CO2 gasification of biochars prepared from Brazilian agro-industrial residues: effect of biomass indigenous mineral content. Biomass Convers Biorefinery 2021. https://doi.org/10.1007/s13399-021-01671-y.

[47] Cay Hakan, Duman Gozde, Yanik Jale. Two-step Gasification of Biochar for Hydrogen-Rich Gas Production: Effect of the Biochar Type and Catalyst. Energy Fuels 2019;33(8):7398–405. https://doi.org/10.1021/acs.energyfuels.9b0135410.1021/acs.energyfuels.9b01354.s001.

[48] Chaiklangmuang Suparin, Kurosawa Keisuke, Li Liuyun, Morishita Kayoko, Takarada Takayuki. Thermal degradation behavior of coffee residue in comparison with biomasses and its product yields from gasification. J Energy Inst 2015;88(3):323–31. https://doi.org/10.1016/j.joei.2014.08.001.

[49] Ferreira Sérgio, Monteiro Eliseu, Brito Paulo, Castro Carlos, Calado Luís, Vilarinho Cândida. Experimental analysis of brewers' spent grains steam gasification in an allothermal batch reactor. Energies 2019;12(5):912. https://doi.org/10.3390/en12050912.

[50] Mendoza Martinez Clara Lisseth, Saari Jussi, Melo Yara, Cardoso Marcelo, de Almeida Gustavo Matheus, Vakkilainen Esa. Evaluation of thermochemical routes for the valorization of solid coffee residues to produce biofuels: A Brazilian case. Renew Sustain Energy Rev 2021;137:110585. https://doi.org/10.1016/j.rser.2020.110585.

[51] Miranda Mara Rúbia da Silva, Veras Carlos Alberto Gurgel, Ghesti Grace Ferreira. Charcoal production from waste pequi seeds for heat and power generation. Waste Manag 2020;103:177–86. https://doi.org/10.1016/j.wasman.2019.12.025.

[52] Guimarães Munique Gonçalves, Evaristo Rafael Benjamin Werneburg, de Mendonça Brasil Augusto César, Ghesti Grace Ferreira. Green energy technology from buriti (Mauritia flexuosa L. f.) for Brazilian agro-extractive communities. SN Appl. Sci. 2021;3(3). https://doi.org/10.1007/s42452-021-04278-0.

[53] Gong M, Nanda S, Hunter HN, Zhu W, Dalai AK, Kozinski JA. Lewis acid catalyzed gasification of humic acid in supercritical water. Catal Today 2017;291:13–23. https://doi.org/10.1016/j.cattod.2017.02.017.

[54] Zhang Yaning, Li Liqing, Xu Pingfei, Liu Bingxu, Shuai Yong, Li Bingxi. Hydrogen production through biomass gasification in supercritical water: A review from exergy aspect. Int J Hydrogen Energy 2019;44(30):15727–36. https://doi.org/10.1016/j.ijhydene.2019.01.151.

[55] Zhang Yaning, Xu Pingfei, Liang Shuang, Liu Bingxu, Shuai Yong, Li Bingxi. Exergy analysis of hydrogen production from steam gasification of biomass: A review. Int J Hydrogen Energy 2019;44(28):14290–302. https://doi.org/10.1016/j.ijhydene.2019.02.064.

[56] He Zhen, Zhang Fan, Tu Ren, Jia Zhiwen, Cheng Shuchao, Sun Yan, et al. The influence of torrefaction on pyrolysed biomass: The relationship of bio-oil composition with the torrefaction severity. Bioresour Technol 2020;314:123780. https://doi.org/10.1016/j.biortech.2020.123780.

[57] Adánez-Rubio I, Ferreira R, Rio T, Alzueta MU, Costa M. Soot and char formation in the gasification of pig manure in a drop tube reactor. Fuel 2020;281:118738. https://doi.org/10.1016/j.fuel.2020.118738.

[58] Ferreiro AI, Segurado R, Costa M. Modelling soot formation during biomass gasification. Renew Sustain Energy Rev 2020;134:110380. https://doi.org/10.1016/j.rser.2020.110380.

[59] Ferreira Ricardo, Petrova Tsvetelina, Ferreira Ana F, Costa Mário, Inaydenova Iliyana, Atanasova-Vladimirova Stela, et al. Size-Segregated Particulate Matter from Gasification of Bulgarian Agro-Forest Biomass Residue. Energies 2021;14(2):385. https://doi.org/10.3390/en14020385.

[60] Franco C, Pinto F, Gulyurtlu I, Cabrita I. The study of reactions influencing the biomass steam gasification process. Fuel 2003;82(7):835–42. https://doi.org/10.1016/S0016-2361(02)00313-7.

[61] Parvez AM, Mujtaba IM, Wu T. Energy, exergy and environmental analyses of conventional, steam and CO2-enhanced rice straw gasification. Energy 2016;94:579–88. https://doi.org/10.1016/j.energy.2015.11.022.

[62] Hu Yisheng, Pang Kang, Cai Longhao, Liu Zhibin. A multi-stage co-gasification system of biomass and municipal solid waste (MSW) for high quality syngas production. Energy 2021;221:119639. https://doi.org/10.1016/j.energy.2020.119639.

[63] Chen WH, Chen CJ, Hung CI, Shen CH, Hsu HW. A comparison of gasification phenomena among raw biomass, torrefied biomass and coal in an entrained-flow reactor. Appl Energy 2013;112:421–30. https://doi.org/10.1016/j.apenergy.2013.01.034.

[64] Waldheim, L. Nilsson T. HEATING VALUE OF GASES FROM Report prepared for : IEA Bioenergy Agreement, English 2001.

[65] Xiang Xianan, Gong Guangcai, Wang Chenhua, Cai Ninghua, Zhou Xuehua, Li Yongsuo. Exergy analysis of updraft and downdraft fixed bed gasification of village-level solid waste. Int J Hydrogen Energy 2021;46(1):221–33. https://doi.org/10.1016/j.ijhydene.2020.09.247.

[66] Zhang Y, Zhao Y, Gao X, Li B, Huang J. Energy and exergy analyses of syngas produced from rice husk gasification in an entrained flow reactor. J Clean Prod 2015;95:273–80. https://doi.org/10.1016/j.jclepro.2015.02.053.

[67] Zhang Y, Li B, Li H, Zhang B. Exergy analysis of biomass utilization via steam gasification and partial oxidation. Thermochim Acta 2012;538:21–8. https://doi.org/10.1016/j.tca.2012.03.013.

[68] Caglar Basar, Tavsanci Duygu, Biyik Emrah. Multiparameter-based product, energy and exergy optimizations for biomass gasification. Fuel 2021;303:121208. https://doi.org/10.1016/j.fuel.2021.121208.

[69] Ferreira Ana F, Ribau João P, Costa Mário. A decision support method for biochars characterization from carbonization of grape pomace. Biomass Bioenergy 2021;145:105946. https://doi.org/10.1016/j.biombioe.2020.105946.

[70] Silveira Edgar A, Lin Bo-Jhih, Colin Baptiste, Chaouch Mounir, Pétrissans Anélie, Rousset Patrick, et al. Heat treatment kinetics using three-stage approach for sustainable wood material production. Ind Crops Prod 2018;124:563–71. https://doi.org/10.1016/j.indcrop.2018.07.045.

[71] Silveira Edgar A, Galvão Luiz Gustavo Oliveira, Sá Isabella A, Silva Bruno F, Macedo Lucélia, Rousset Patrick, et al. Effect of torrefaction on thermal behavior and fuel properties of Eucalyptus grandis macro-particulates. J Therm Anal Calorim 2019;138(5):3645–52. https://doi.org/10.1007/s10973-018-07999-4.

[72] A. Silveira Edgar, Oliveira Galvão Luiz Gustavo, Alves de Macedo Lucélia, A. Sá Isabella, S. Chaves Bruno, Girão de Morais Marcus Vinícius, et al. Thermo-Acoustic Catalytic Effect on Oxidizing Woody Torrefaction. Processes 2020;8:1361.;8(11):1361. https://doi.org/10.3390/pr8111361.

[73] Silveira Edgar A, Macedo Lucélia A, Rousset Patrick, Candelier Kevin, Galvão Luiz Gustavo O, Chaves Bruno S, et al. A potassium responsive numerical path to model catalytic torrefaction kinetics. Energy 2022;239:122208. https://doi.org/10.1016/j.energy.2021.122208.

[74] Lin Bo-Jhih, Silveira Edgar A, Colin Baptiste, Chen Wei-Hsin, Lin Yu-Ying, Leconte François, et al. Modeling and prediction of devolatilization and elemental composition of wood during mild pyrolysis in a pilot-scale reactor. Ind Crops Prod 2019;131:357–70. https://doi.org/10.1016/j.indcrop.2019.01.065.

[75] Chen WH, Cheng CL, Show PL, Ong HC. Torrefaction performance prediction approached by torrefaction severity factor. Fuel 2019;251:126–35. https://doi.org/10.1016/j.fuel.2019.04.047.

[76] Lu KM, Lee WJ, Chen WH, Liu SH, Lin TC. Torrefaction and low temperature carbonization of oil palm fiber and eucalyptus in nitrogen and air atmospheres. Bioresour Technol 2012;123:98–105. https://doi.org/10.1016/j.biortech.2012.07.096.

[77] Zhang C, Ho SH, Chen WH, Fu Y, Chang JS, Bi X. Oxidative torrefaction of biomass nutshells: Evaluations of energy efficiency as well as biochar transportation and storage. Appl Energy 2019;235:428–41. https://doi.org/10.1016/j.apenergy.2018.10.090.

[78] Galvão LGOBSC, Morais MVG de, Vale AT do V, Caldeira-Pires A, Rousset P, Silveira EA. Combined thermo-acoustic upgrading of solid fuel: experimental and numerical investigation. 28th Eur. Biomass Conf. Exhib., 2020, p. 6–9. https://doi.org/10.5071/28thEUBCE2020-3DO.6.2.

[79] Santanna MS, Silveira EA, Macedo L, Galvão LGO, Caldeira-Pires A. Torrefaction of lignocellulosic municipal solid waste: thermal upgrade for energy use. 28th Eur. Biomass Conf. Exhib., Marseille 2020:188–91. https://doi.org/10.5071/28thEUBCE2020-1DV.1.34.

[80] Silveira EA, de Morais MVG, Rousset P, Caldeira-Pires A, Pétrissans A, Galvão LGO. Coupling of an acoustic emissions system to a laboratory torrefaction reactor. J Anal Appl Pyrolysis 2018;129:29–36. https://doi.org/10.1016/j.jaap.2017.12.008.

[81] Paniagua Bermejo S, Prado-Guerra A, García Pérez AI, Calvo Prieto LF. Study of quinoa plant residues as a way to produce energy through thermogravimetric analysis and indexes estimation. Renew Energy 2020;146:2224–33. https://doi.org/10.1016/j.renene.2019.08.04.

[82] Mureddu M, Dessì F, Orsini A, Ferrara F, Pettinau A. Air- and oxygen-blown characterization of coal and biomass by thermogravimetric analysis. Fuel 2018;212:626–37. https://doi.org/10.1016/j.fuel.2017.10.005.

[83] Protásio Thiago de Paula, Lima Michael Douglas Roque, Scatolino Mário Vanoli, de Araújo Ana Clara Caxito, de Figueiredo Izabel Cristina Rodrigues, Bufalino Lina, et al. Insights in quantitative indexes for better grouping and classification of Eucalyptus clones used in combustion and energy cogeneration processes in Brazil. Biomass Bioenergy 2020;143:105835. https://doi.org/10.1016/j.biombioe.2020.105835.

[84] Li Xiang-guo, Ma Bao-guo, Xu Li, Hu Zhen-wu, Wang Xin-gang. Thermogravimetric analysis of the co-combustion of the blends with high ash coal and waste tyres. Thermochim Acta 2006;441(1):79–83. https://doi.org/10.1016/j.tca.2005.11.044.

[85] Zhang Y, Guo Y, Cheng F, Yan K, Cao Y. Investigation of combustion characteristics and kinetics of coal gangue with different feedstock properties by thermogravimetric analysis. Thermochim Acta 2015;614:137–48. https://doi.org/10.1016/j.tca.2015.06.018.

[86] Deb K. Multi-objective Optimisation Using Evolutionary Algorithms: An Introduction. Multi-objective Evol. Optim. Prod. Des. Manuf., London: Springer London; 2011, p. 3–34. https://doi.org/10.1007/978-0-85729-652-8_1.

[87] Prasertcharoensuk Phuet, Bull Steve J, Arpornwichanop Amornchai, Phan Anh N. Sustainable Hydrogen Production from Waste Wood and CO2. Ind Eng Chem Res 2021;60(33):12362–76. https://doi.org/10.1021/acs.iecr.1c01810.

[88] Hernández JJ, Aranda G, Barba J, Mendoza JM. Effect of steam content in the air-steam flow on biomass entrained flow gasification. Fuel Process Technol 2012;99:43–55. https://doi.org/10.1016/j.fuproc.2012.01.030.

[89] Dupont Capucine, Boissonnet Guillaume, Seiler Jean-Marie, Gauthier Paola, Schweich Daniel. Study about the kinetic processes of biomass steam gasification. Fuel 2007;86(1-2):32–40. https://doi.org/10.1016/j.fuel.2006.06.011.

[90] Klinghoffer NB, Castaldi MJ. Gasifi cation and pyrolysis of municipal solid waste (MSW). 2013. https://doi.org/10.1533/9780857096364.2.146.

[91] Fremaux S, Beheshti SM, Ghassemi H, Shahsavan-Markadeh R. An experimental study on hydrogen-rich gas production via steam gasification of biomass in a research-scale fluidized bed. Energy Convers Manag 2015;91:427–32. https://doi.org/10.1016/j.enconman.2014.12.048.

[92] He Maoyun, Xiao Bo, Liu Shiming, Guo Xianjun, Luo Siyi, Xu Zhuanli, et al. Hydrogen-rich gas from catalytic steam gasification of municipal solid waste (MSW): Influence of steam to MSW ratios and weight hourly space velocity on gas production and composition. Int J Hydrogen Energy 2009;34(5):2174–83. https://doi.org/10.1016/j.ijhydene.2008.11.115.

[93] Septien S, Valin S, Peyrot M, Spindler B, Salvador S. Influence of steam on gasification of millimetric wood particles in a drop tube reactor: Experiments and modelling. Fuel 2013;103:1080–9. https://doi.org/10.1016/j.fuel.2012.09.011.

[94] Billaud J, Valin S, Peyrot M, Salvador S. Influence of H 2 O , CO 2 and O 2 addition on biomass gasification in entrained flow reactor conditions : Experiments and modelling 2016;166:166–78. https://doi.org/10.1016/j.fuel.2015.10.046.

[95] Pradhan D, Singh RK, Bendu H, Mund R. Pyrolysis of Mahua seed (Madhuca indica) – Production of biofuel and its characterization. Energy Convers Manag 2016;108:529–38. https://doi.org/10.1016/j.enconman.2015.11.042.

[96] Guerrero Marta, Ruiz M Pilar, Millera Ángela, Alzueta María U, Bilbao Rafael. Characterization of biomass chars formed under different devolatilization conditions: Differences between rice husk and Eucalyptus. Energy Fuels 2008;22(2):1275–84. https://doi.org/10.1021/ef7005589.

[97] Vakalis Stergios, Moustakas Konstantinos, Benedetti Vittoria, Cordioli Eleonora, Patuzzi Francesco, Loizidou Maria, et al. The "COFFEE BIN" concept: centralized collection and torrefaction of spent coffee grounds. Environ Sci Pollut Res 2019; 26(35):35473–81. https://doi.org/10.1007/s11356-019-04919-3.

[98] McNutt J, He Sophia Q. Spent coffee grounds: A review on current utilization. J Ind Eng Chem 2019;71:78–88. https://doi.org/10.1016/j.jiec.2018.11.054.

[99] Fontana Izabela B, Peterson Michael, Cechinel Maria Alice P. Application of brewing waste as biosorbent for the removal of metallic ions present in groundwater and surface waters from coal regions. J Environ Chem Eng 2018;6 (1):660–70.

[100] Morin M, Pécate S, Hémati M, Kara Y. Pyrolysis of biomass in a batch fluidized bed reactor: Effect of the pyrolysis conditions and the nature of the biomass on the physicochemical properties and the reactivity of char. J Anal Appl Pyrolysis 2016; 122:511–23. https://doi.org/10.1016/j.jaap.2016.10.002.

[101] Xiong S, Zhang S, Wu Q, Guo X, Dong A, Chen C. Investigation on cotton stalk and bamboo sawdust carbonization for barbecue charcoal preparation. Bioresour Technol 2014;152:86–92. https://doi.org/10.1016/j.biortech.2013.11.005.

[102] Xinjie Liao, Singh Surjit, Yang Haiping, Wu Chunfei, Zhang Shihong. A thermogravimetric assessment of the tri-combustion process for coal, biomass and polyethylene. Fuel 2021;287:119355. https://doi.org/10.1016/j.fuel.2020.119355.

[103] Wnorowska Joanna, Ciukaj Szymon, Kalisz Sylwester. Thermogravimetric analysis of solid biofuels with additive under air atmosphere. Energies 2021;14 (8):2257. https://doi.org/10.3390/en14082257.

[104] Protásio T de P, Junior MG, Mirmehdi S, Trugilho PF, Napoli A, Knovack KM. Combustão da biomassa E do carvão vegetal da casca do coco babaçu. Cerne 2017;23:1–10. https://doi.org/10.1590/01047760201723012202.

[105] Qian Wei, Xie Qiang, Huang Yuyi, Dang Jiatao, Sun Kaidi, Yang Qian, et al. Combustion characteristics of semicokes derived from pyrolysis of low rank bituminous coal. Int J Min Sci Technol 2012;22(5):645–50. https://doi.org/10.1016/j.ijmst.2012.08.009.

[106] Moon C, Sung Y, Ahn S, Kim T, Choi G, Kim D. Effect of blending ratio on combustion performance in blends of biomass and coals of different ranks. Exp Therm Fluid Sci 2013;47:232–40. https://doi.org/10.1016/j.expthermflusci.2013.01.019.